Chapter 3: Free Vibration of the Breakwater

3.1 Introduction

Before conducting forcing analyses on the breakwater, a free vibration study is necessary. This chapter will describe the analysis conducted to determine the natural frequencies of the structure and its modes of vibration, which are necessary to understand the behavior of the breakwater when undergoing wave forcing. Initiating large displacements on the structure will show the effects of the nonlinearities of the problem. A study of the effects of linear damping will conclude this chapter.

3.2 Linearized Equations of Motion

To find the natural vibration frequencies and modes of the structure, small motions about the equilibrium of the cylinder must be assumed. This assumption allows the use of the linearized EOM's, which are much simpler than the complete nonlinear EOM's. The linear EOM's are presented in Equations 3.1-3.6, based on Mays et al. (1999), in nondimensional form modified for the dimensions and axes of this breakwater, where the subscript i has been dropped for the stiffness and natural length because they are the same for each mooring line:

$$m\ddot{x}_c + 4k\left(1 - \frac{\tilde{l}}{\tilde{l}_o}\right)x_c + \left(4\tilde{a}^2 x - 4\tilde{a}y_{c\_eq}\frac{\tilde{L}}{2}\psi\right)\frac{k\tilde{l}}{\tilde{l}_o^3} = 0 \tag{3.1}$$

$$m\ddot{y}_c + 4k\left(1 - \frac{\tilde{l}}{\tilde{l}_o}\right)y_c + 4y_{c\_eq}^2\frac{k\tilde{l}}{\tilde{l}_o^3}y_c = 0 \tag{3.2}$$

$$m\ddot{z}_c + 4k\left(1 - \frac{\tilde{l}}{\tilde{l}_o}\right)z_c + \left(4\tilde{b}^2 z_c + 4\tilde{b}ry_{c\_eq}\phi\right)\frac{k\tilde{l}}{\tilde{l}_o^3} = 0 \tag{3.3}$$

$$i_{zz}\ddot{\psi} + 4k\left(1 - \frac{\tilde{l}}{\tilde{l}_o}\right)\frac{\tilde{L}}{2}\left(\frac{\tilde{L}}{2} + \tilde{a}\right)\psi + 4\frac{\tilde{L}}{2}y_{c\_eq}\left(-\tilde{a}x_c + \frac{\tilde{L}}{2}y_{c\_eq}\psi\right)\frac{k\tilde{l}}{\tilde{l}_o^3} = 0 \tag{3.4}$$

$$i_{yy}\ddot{\theta} + 4k\left(1 - \frac{\tilde{l}}{\tilde{l}_o}\right)\left[\frac{\tilde{L}}{2}\left(\frac{\tilde{L}}{2} + \tilde{a}\right) + r\left(r + \tilde{b}\right)\right]\theta + 4\left(\frac{\tilde{L}}{2}\tilde{b} - r\tilde{a}\right)\frac{k\tilde{l}}{\tilde{l}_o^3}\theta = 0 \tag{3.5}$$

$$i_{xx}\ddot{\phi} + 4k\left(1 - \frac{\tilde{l}}{\tilde{l}_o}\right)r\left(r + \tilde{b}\right)\phi + 4ry_{c\_eq}\left(\tilde{b}z_c + ry_{c\_eq}\phi\right)\frac{k\tilde{l}}{\tilde{l}_o^3} = 0 \tag{3.6}$$

3.3 Natural Vibration Frequencies and Modes of the Breakwater

3.3.1 Standard Case

The linear EOM's can be put in matrix form as an eigenvalue problem to solve for the natural frequencies and mode shapes of the structure. Although the problem involves six degrees of freedom (DOFs), a 6x6 matrix can be avoided because the linear equations have limited coupling. For instance, notice that Equations 3.2 and 3.5 only involve y and θ, respectively; therefore, they can be treated as single-degree-of-freedom (SDF) problems. Equation 3.2 thus indicates that one of the structure's vibration modes will be heave only, while Equation 3.5 describes a mode of solely yaw motion. Further simplifying the problem is the fact that Equations 3.1 and 3.4 are coupled through the x and ψ variables, which implies that there will be two modes involving both surge and pitch. Equations 3.3 and 3.6 are coupled through z and ϕ, meaning that the remaining two modes of vibration will only involve sway and roll. These simplifications will lead to two independent SDF systems and two eigenvalue problems with 2x2 matrices each.

First the SDF systems will be solved. Equations 3.2 and 3.5 can each be represented in their general form as

$$m\ddot{u} + ku = 0 \tag{3.7}$$

where u represents a general variable, y for the heave mode and θ for the yaw mode. In this SDF case, the natural frequency is simply

$$\tilde{\omega}_n = \sqrt{k/m} \tag{3.8}$$

Therefore, for the standard case ($\tilde{a} = \tilde{b} = 2$, $\tilde{R} = 1$, $\tilde{L} = 6$, and $\tilde{l} = 4$), the natural frequencies for the two SDF problems are:

heave only: $\tilde{\omega}_n = 10.03$ (3.9)

yaw only: $\tilde{\omega}_n = 7.948$ (3.10)

For the two multiple-degree-of-freedom (MDF) systems, the generalized matrix form of the coupled EOM's is

$$[M]\ddot{\mathbf{u}} + [K]\mathbf{u} = 0 \tag{3.11}$$

The variables that **u** represents for the surge and pitch case are

$$\mathbf{u} = \begin{bmatrix} x \\ \psi \end{bmatrix} \tag{3.12}$$

The inertia and stiffness matrices are built from Equations 3.1 and 3.4 and become

$$[M] = \begin{bmatrix} 1 & 0 \\ 0 & 3.25 \end{bmatrix} \tag{3.13}$$

$$[K] = \begin{bmatrix} 50.09 & -211.8 \\ -211.8 & 906.9 \end{bmatrix} \tag{3.14}$$

[M] and [K] are positive definite and therefore the eigenvalues must be real and positive. From the determinant

$$\left|K - \tilde{\omega}_n^2 M\right| = 0 \tag{3.15}$$

the eigenvalues become

$$\left[\tilde{\omega}_n^2\right] = \begin{bmatrix} 0.5453 \\ 328.6 \end{bmatrix} \tag{3.16}$$

which yields the following natural frequencies and the normalized eigenvector matrix, **u**:

$$\left[\tilde{\omega}_n\right] = \begin{bmatrix} 0.7385 \\ 18.13 \end{bmatrix} \tag{3.17}$$

$$\mathbf{u} = \begin{bmatrix} 1 & 1 \\ 0.2340 & -1.315 \end{bmatrix} \tag{3.18}$$

where the first column of **u** corresponds to the lower frequency. The eigenvectors were normalized so that the translation element was unity. The results for the sway and roll case are presented below and were derived from the same process used above:

$$[M] = \begin{bmatrix} 1 & 0 \\ 0 & 0.5 \end{bmatrix} \tag{3.19}$$

$$[K] = \begin{bmatrix} 50.09 & 70.59 \\ 70.59 & 10.12 \end{bmatrix} \tag{3.20}$$

$$\left[\tilde{\omega}_n^2\right] = \begin{bmatrix} 0.7007 \\ 251.9 \end{bmatrix} \tag{3.21}$$

$$\left[\tilde{\omega}_n\right] = \begin{bmatrix} 0.8371 \\ 15.87 \end{bmatrix} \tag{3.22}$$

$$\mathbf{u} = \begin{bmatrix} 1 & 1 \\ -0.6997 & 2.858 \end{bmatrix} \tag{3.23}$$

The six modes of vibration with their corresponding nondimensional and dimensional frequencies and periods are listed in Table 3.1. The subscript j in the table denotes the j^{th} mode of vibration and T_j is its period. Drawings of the mode shapes are included in Figures 3.1-3.6 with the eigenvector ratios being drawn to scale, where r is radians. As seen in Table 3.1, the lowest natural frequency for this system corresponds to surge with "forward pitch" (i.e., surge and pitch are in phase). Figure 3.1 shows that the cylinder moves in the surge direction and has a relatively modest forward pitch rotation. The second mode of vibration is sway with a small amount of "backward roll" (i.e., sway and roll are out of phase), as shown in Figure 3.2. Out of the six natural frequencies of this structure, these two are the only ones with frequencies that could match up to realistic wave forces. Figures 3.3 and 3.4 qualitatively describe the SDF motions of the third and fourth modes. The third natural frequency is for the vibration mode of yaw motion only. This frequency is significantly higher than the first two frequencies. The fourth mode of vibration involves only heave motion and does not take as great of a jump in value from the third frequency as from the second to third. The last two natural frequencies are significantly higher than the third and fourth frequencies. The fifth frequency involves sway with a large amount of "forward roll," as seen in Figure 3.5. Figure 3.6 displays the great amount of "backward pitch" that is coupled with surge in the sixth mode of vibration.

Table 3.1. Natural Frequencies and Periods, Standard Case

j	Mode	$\tilde{\omega}_j$	$\tilde{T}_j$	ω_j (rad/s)	T_j (s)
1	Surge with Forward Pitch	0.7385	8.509	1.873	3.354
2	Sway with Backward Roll	0.8371	7.506	2.123	2.959
3	Yaw	7.948	0.7906	20.16	0.3117
4	Heave	10.03	0.6267	25.43	0.2470
5	Sway with Forward Roll	15.87	0.3959	40.26	0.1561
6	Surge with Backward Pitch	18.13	0.3466	45.98	0.1366

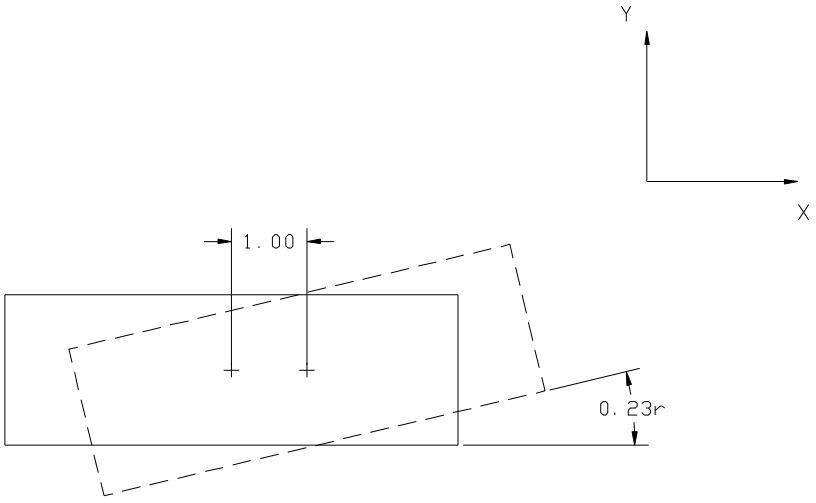

Figure 3.1. 1st Mode: Surge with Forward Pitch

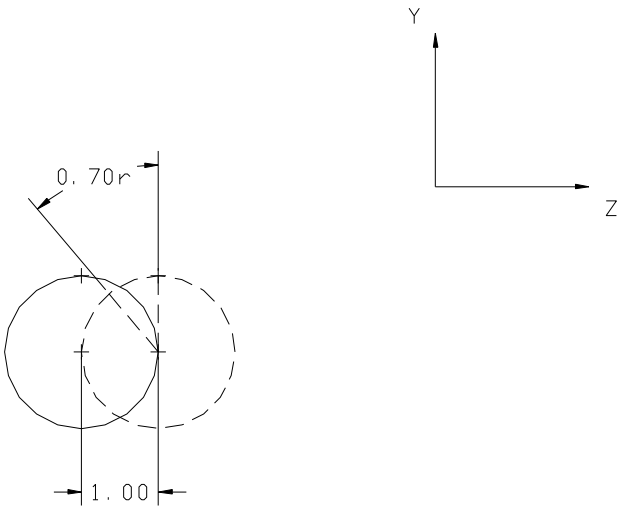

Figure 3.2. 2nd Mode: Sway with Backward Roll

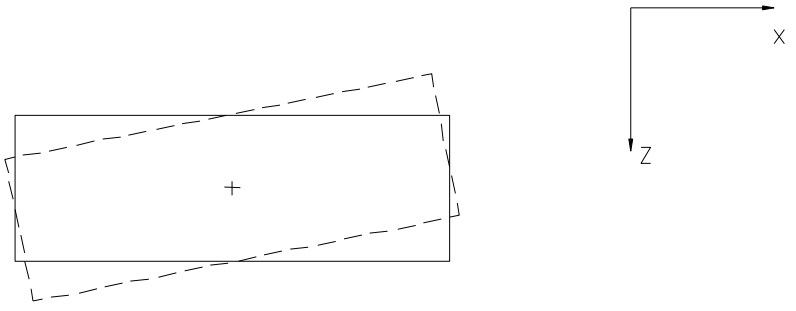

Figure 3.3. 3rd Mode: Yaw Only

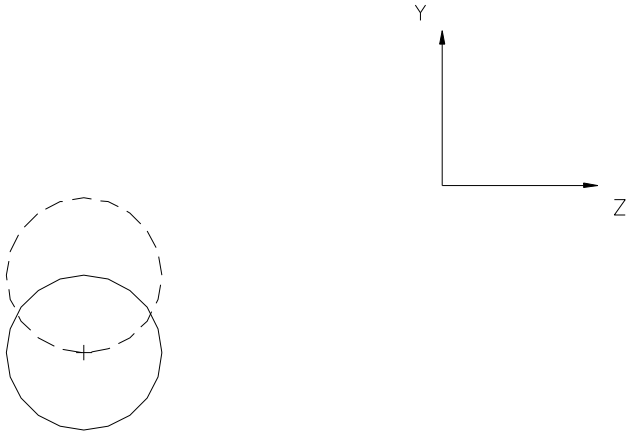

Figure 3.4. 4th Mode: Heave Only

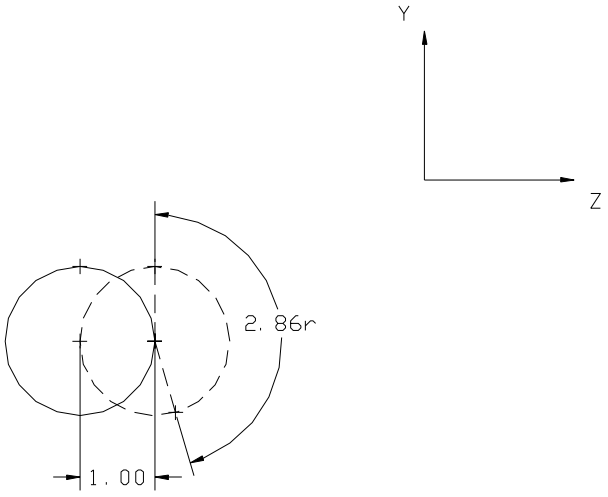

Figure 3.5. 5th Mode: Sway with Forward Roll

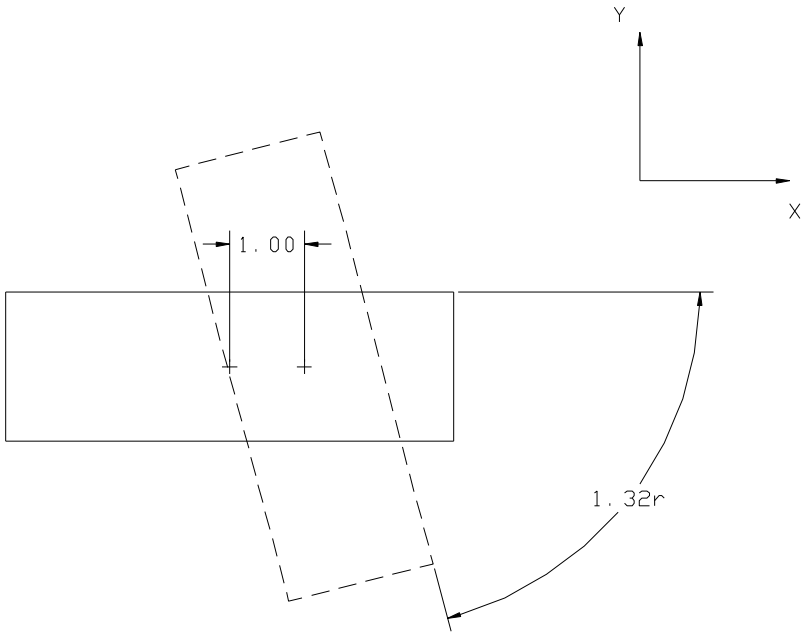

Figure 3.6. 6th Mode: Surge with Backward Pitch

3.3.2 Special Case

If the net buoyancy is zero ($\tilde{w}$ = 0), the breakwater is in its equilibrium position with the springs unstretched, i.e., in their natural length. By using the same methods as in Section 3.3.1, the natural frequencies and eigenvectors can be found for this case. Simplifying Equations 3.1-3.6 by setting the equilibrium length, $\tilde{l}_o$, equal to the natural length, $\tilde{l}$, general equations for the frequencies and corresponding modes can be found, which are shown in Equations 3.24-3.33. The first two frequencies corresponding to surge and pitch, and sway and roll are zero. Notice that the modes do not depend on the stiffness of the springs.

Heave: $$\tilde{\omega}_n^2 = 4y_{c\_eq}^2 \frac{k}{\tilde{l}^2} \tag{3.24}$$

Yaw: $$i_{yy}\tilde{\omega}_n^2 = 4\left(\frac{\tilde{L}}{2}\tilde{b} - r\tilde{a}\right)^2 \frac{k}{\tilde{l}^2} \quad (3.25)$$

Surge/Pitch: $$\tilde{\omega}_n = 0 \quad (3.26)$$

$$\tilde{a}x = \beta\psi \quad (3.27)$$

$$\tilde{\omega}_n^2 = \frac{4k}{\tilde{l}^2}\left(\tilde{a}^2 + \frac{\beta^2}{i_{zz}}\right) \quad (3.28)$$

$$\beta x = -\tilde{a}i_{zz}\psi \quad (3.29)$$

Sway/Roll: $$\tilde{\omega}_n = 0 \quad (3.30)$$

$$\tilde{b}z = \gamma\phi \quad (3.31)$$

$$\tilde{\omega}_n^2 = \frac{4k}{\tilde{l}^2}\left(\tilde{b}^2 + \frac{\gamma^2}{i_{xx}}\right) \quad (3.32)$$

$$\gamma z = \tilde{b}i_{xx}\phi \quad (3.33)$$

where $$\beta = y_{c\_eq}\frac{\tilde{L}}{2} \quad (3.34)$$

$$\gamma = ry_{c\_eq} \quad (3.35)$$

All the same parameters will be used for this investigation, except of course the equilibrium length of the mooring lines. Because the equilibrium length of the springs is known, the equilibrium height can be easily found from Equation 3.36:

$$\tilde{l}_o = 4 = \sqrt{\tilde{a}^2 + \tilde{b}^2 + y_{c\_eq}^2} \quad (3.36)$$

The result is $y_{c\_eq} = \sqrt{8}$. The natural vibration frequencies and modes can then be found and are presented in Table 3.2.

Table 3.2. Natural Frequencies and Periods, Special Case

j	Mode	$\tilde{\omega}_j$	$\tilde{T}_j$	ω_j (rad/s)	T_j (s)
1	Surge with Forward Pitch	0	N/A	0	N/A
2	Sway with Backward Roll	0	N/A	0	N/A
3	Yaw	7.845	0.8010	19.90	0.3157
4	Heave	10.00	0.6283	25.37	0.2477
5	Sway with Forward Roll	15.81	0.3974	40.11	0.1567
6	Surge with Backward Pitch	18.08	0.3475	45.87	0.1370

Thus, the two lowest natural frequencies are zero. Even though the frequencies are zero for the first two modes, the structure still has mode shapes, as shown in the following eigenvectors:

$$\begin{bmatrix} x_c \\ \psi \end{bmatrix}_1 = \begin{bmatrix} 1 \\ 0.2357 \end{bmatrix} \tag{3.37}$$

$$\begin{bmatrix} z_c \\ \phi \end{bmatrix}_2 = \begin{bmatrix} 1 \\ -0.7071 \end{bmatrix} \tag{3.38}$$

Notice that the eigenvectors are very close to those for the standard case. The rest of the natural frequencies for this case are also quite similar to those of the standard case. The remaining two eigenvectors are

$$\begin{bmatrix} z_c \\ \phi \end{bmatrix}_5 = \begin{bmatrix} 1 \\ 2.828 \end{bmatrix} \tag{3.39}$$

$$\begin{bmatrix} x_c \\ \psi \end{bmatrix}_6 = \begin{bmatrix} 1 \\ -1.305 \end{bmatrix} \tag{3.40}$$

3.3.3 Effect of Stiffness on the Natural Frequencies

It is interesting to see the effect that the spring stiffness has on the six natural frequencies. Figures 3.7-3.9 plot the relationships between the natural frequencies and the stiffness for the standard case. The first point demonstrated through this analysis is that the order of the modes does not depend on the stiffness. In other words, the six modes of vibration remained in the same order for every value of k used. Furthermore, the first two natural frequencies are hardly affected by the stiffness if it is sufficiently large. Therefore, the geometry and mass of the breakwater are the main contributors to the structure's first two vibration modes. However, for the remaining four natural frequencies, the stiffness greatly affects their values. As the stiffness increases, the frequencies increase almost linearly if k is sufficiently large. It should also be noted that the third and fourth frequencies remain grouped together and the same occurs with the fifth and sixth frequencies, although they very slowly pull away from each other.

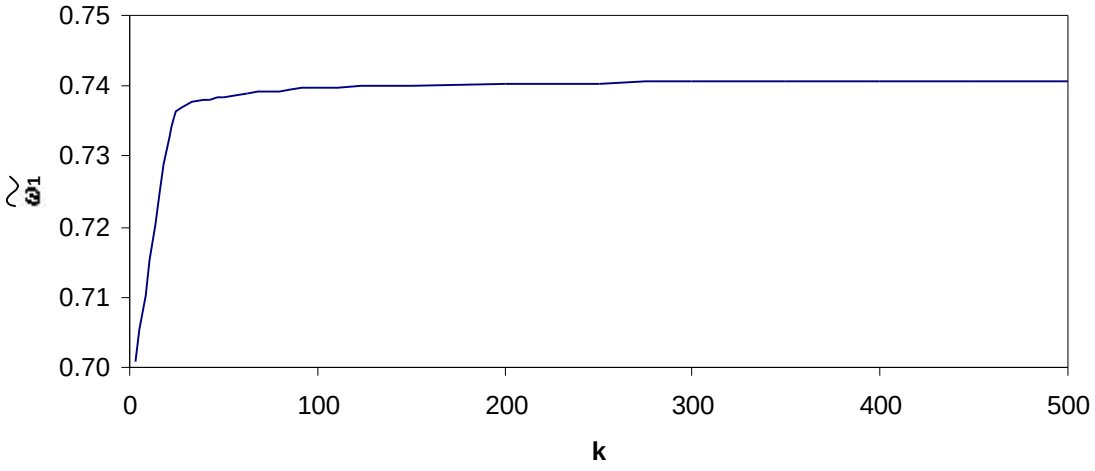

Figure 3.7. 1st Natural Frequency vs. Stiffness

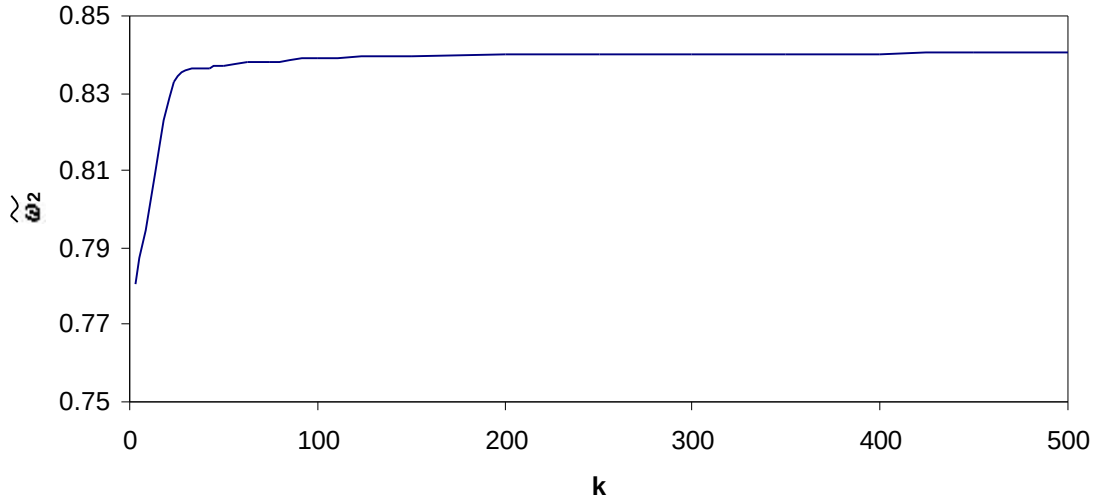

Figure 3.8. 2nd Natural Frequency vs. Stiffness

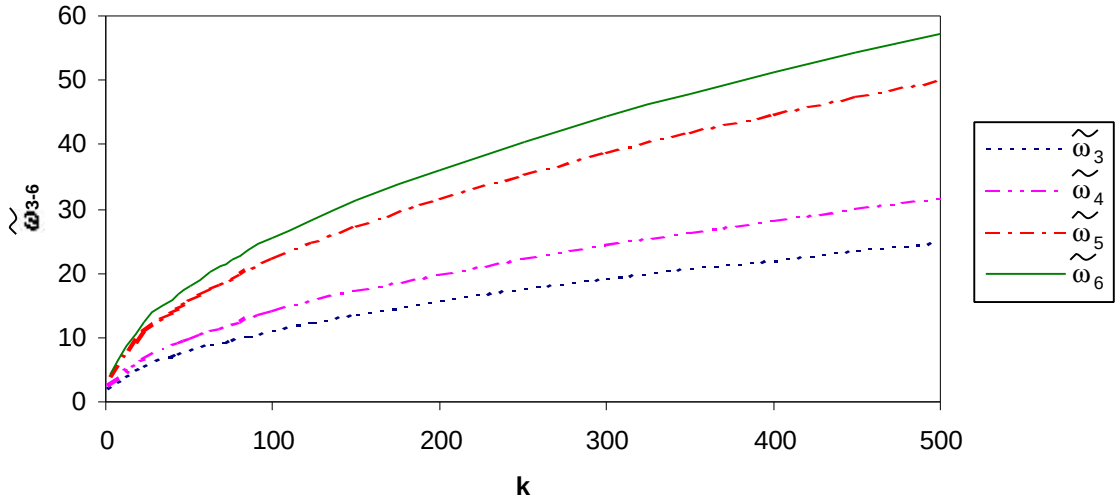

Figure 3.9. 3rd – 6th Natural Frequencies vs. Stiffness

3.4 Verification of Modes with the Computer Model

The knowledge of how the breakwater should behave under undamped free vibration was used to validate the computer program used for future forcing analyses. The procedure used was to apply small initial displacements on the breakwater for each of the six modes of vibration. If the structure remained in its corresponding mode with all other DOFs remaining at their equilibrium values, the program was assumed to be behaving correctly.

3.4.1 Computer Analysis

A FORTRAN program was used to analyze the breakwater for free vibration and a multitude of forcing scenarios. The basic program consists of the nonlinear EOMs, the initial conditions, and all of the parameters of the breakwater. A maximum time limit is defined along with a time step. In order to solve the nonlinear ordinary differential equations, the main program calls a subroutine from the IMSL Math Library called DIVPAG. The six second-order EOM's are written as 12 first-order equations. A loop within the program calls DIVPAG at each time step to solve the equations, in which the displacements and velocities can then be written into an output file. The default integration method in DIVPAG is the Adams-Moulton method, although Gear's BDF method can also be used (IMSL MATH/LIBRARY,1991). Both methods were tested and provided very similar results, and the Adams-Moulton method was chosen. DIVPAG provides error control and allows the user to input the tolerance desired. The error norm that DIVPAG uses is the minimum of the absolute error and the relative error for each time step. The tolerance selected for this research is 1×10^{-10}. Three sample programs are supplied in Appendices A.1-A.3.

One important feature of the program is that it stops when the center of gravity of the cylinder is less than or equal to zero in the heave direction. This assumes that the cylinder has collapsed, even though in reality, it would have collapsed earlier because the bottom of the cylinder would have to hit the ocean floor before the cylinder's center of gravity. Therefore, all of the analyses conducted for this research do not consider the

behavior of the breakwater after it has collapsed. This is later proved to be a valid assumption, because the cylinder only collapses in very extreme cases.

After the data points were generated by DIVPAG, the data was analyzed using Microsoft Excel. Along with calculations, Excel was also used to plot the time histories for the various cases and other types of plots.

3.4.2 Time Histories

For the first mode of the structure, surge with forward pitch, the small initial displacements imposed on the cylinder were $x_o = 0.1$ and $\psi_o = 0.0234$. These values maintain the same ratio as the eigenvector for this mode. Figures 3.10 and 3.11 display the surge and pitch motions vibrating about their equilibrium locations. Notice that the period of the motion for both DOFs is 8.5, which was the period calculated earlier. Furthermore, the amplitude of motion remains constant for both cases, as it should for small free vibration. The four other DOFs were confirmed to stay at their equilibrium position throughout the time of motion.

The remaining modes are similarly presented in Figures 3.12-3.19. For each of the coupled modes (second, fifth, and sixth modes), the ratio of the initial translations to the initial rotations are at the ratios from the eigenvectors derived in Section 3.3.1. The fifth and sixth modes required smaller displacements to model the linear free vibration. Each of the time histories displays simple harmonic motion with each DOF vibrating about its equilibrium position. The periods for each mode match the ones listed in Table 3.1. For each case, all of the DOFs not involved in the mode were verified to have no motion.

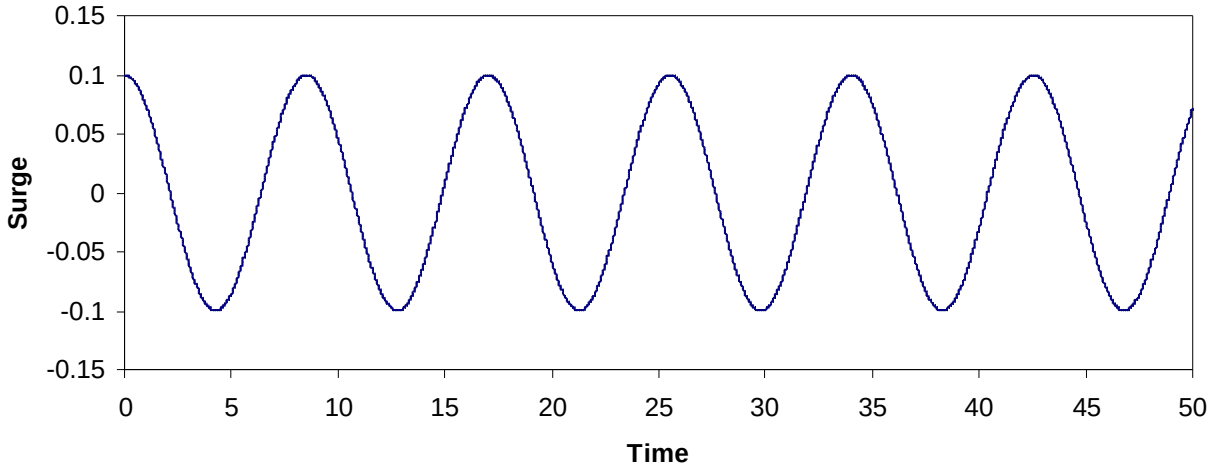

Figure 3.10. x_c, Undamped Free Vibration, 1st Mode: Surge with Forward Pitch

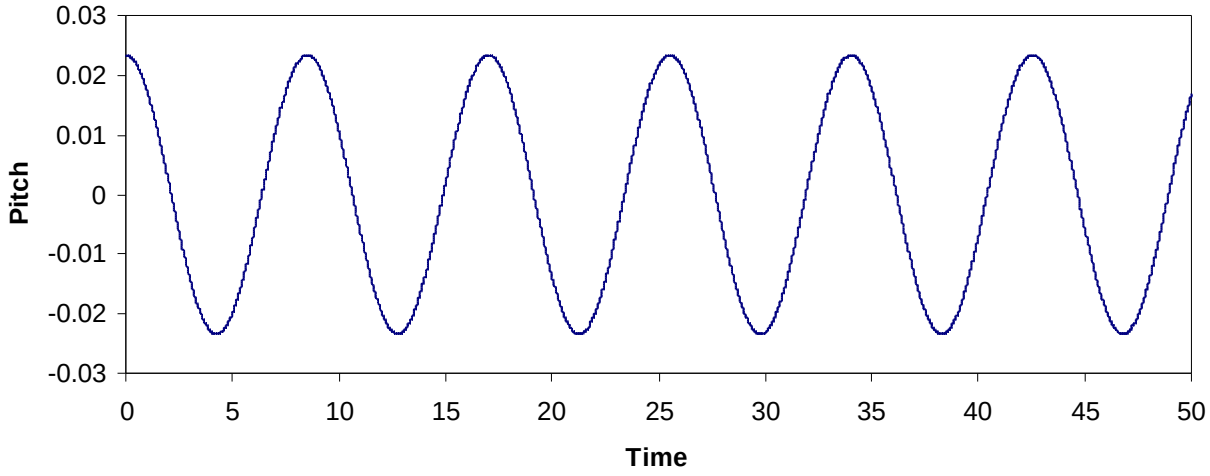

Figure 3.11. y , Undamped Free Vibration, 1st Mode: Surge with Forward Pitch

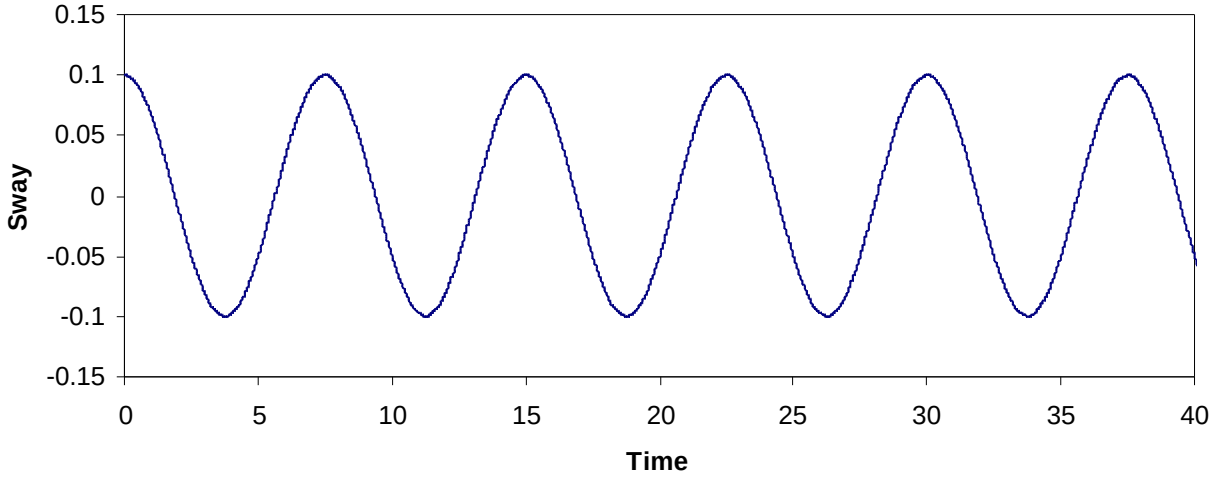

Figure 3.12. z_c, Undamped Free Vibration, 2nd Mode: Sway with Backward Roll

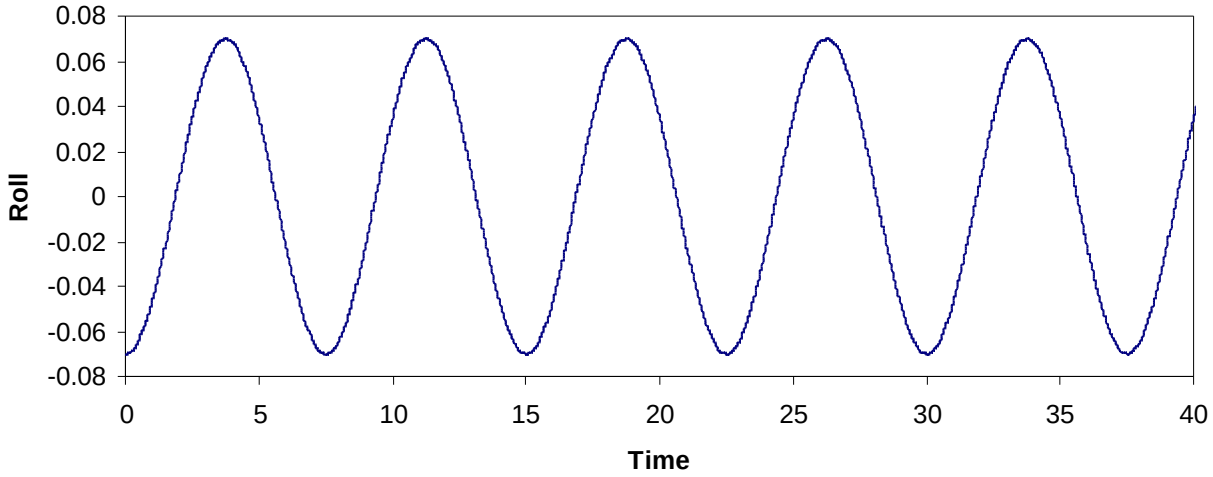

Figure 3.13. f, Undamped Free Vibration, 2nd Mode: Sway with Backward Roll

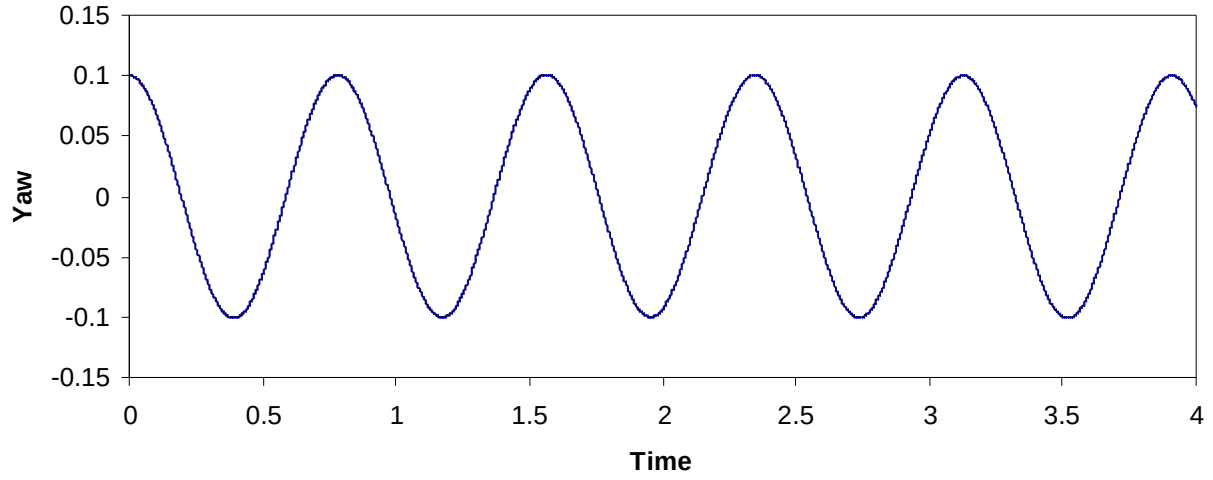

Figure 3.14. q, Undamped Free Vibration, 3rd Mode: Yaw Only

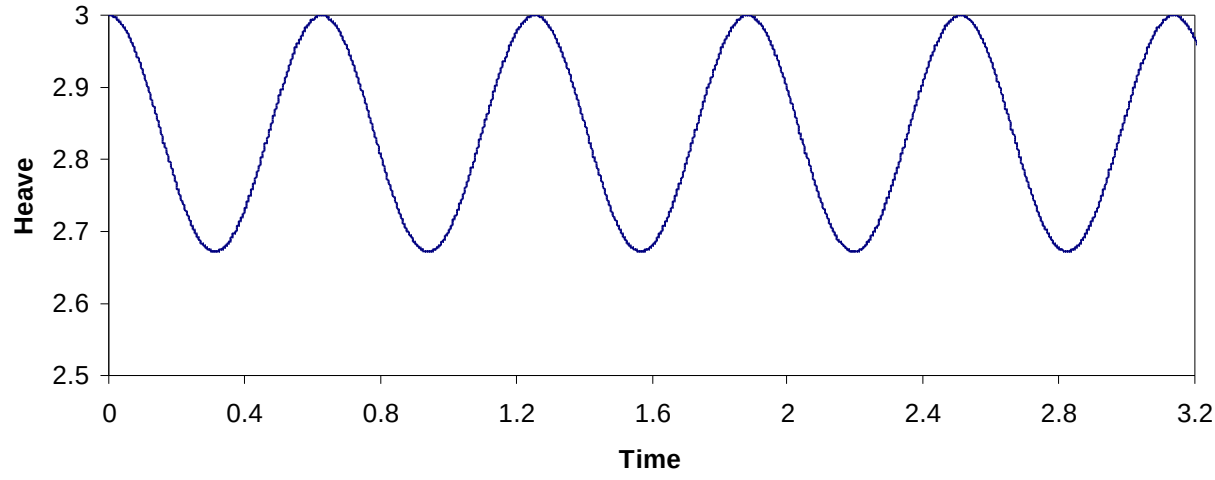

Figure 3.15. y_c, Undamped Free Vibration, 4th Mode: Heave Only

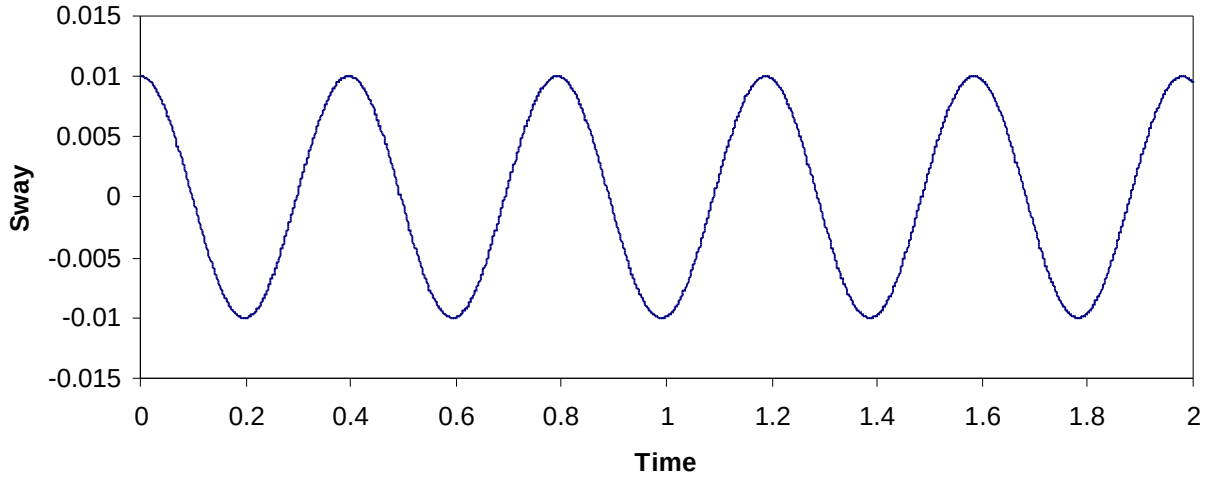

Figure 3.16. z_c, Undamped Free Vibration, 5th Mode: Sway with Forward Roll

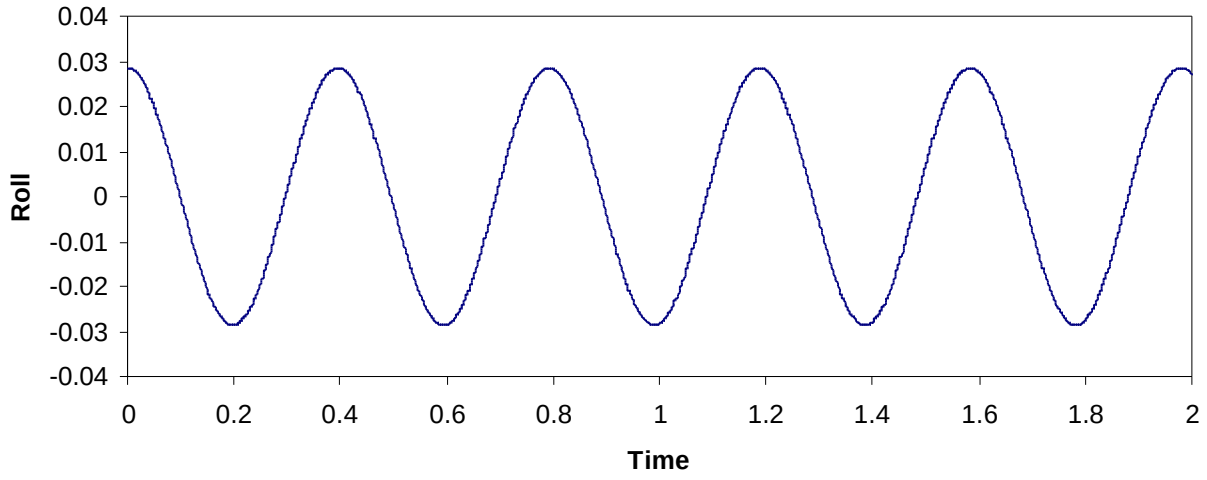

Figure 3.17. f, Undamped Free Vibration, 5th Mode: Sway with Forward Roll

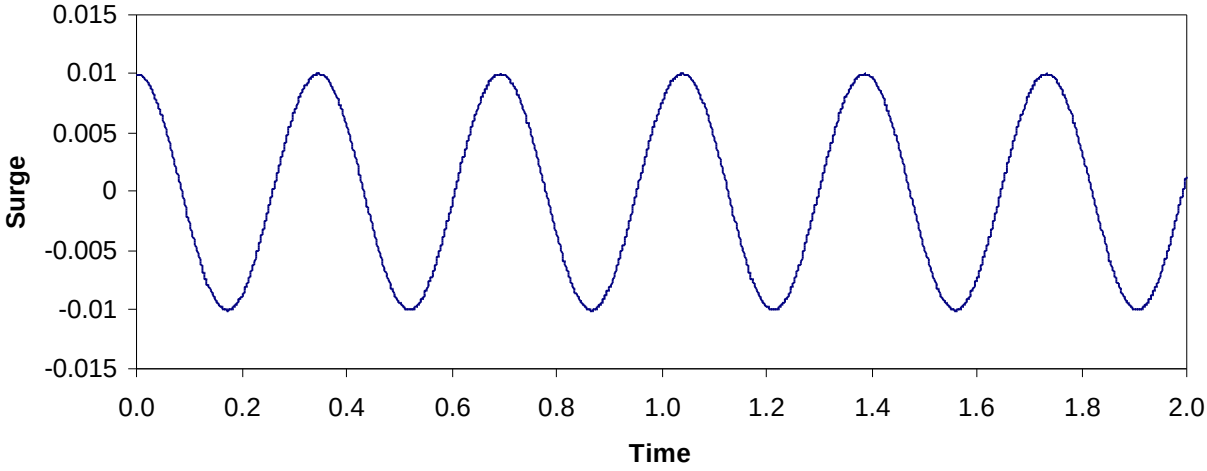

Figure 3.18. x_c, Undamped Free Vibration, 6th Mode: Surge with Backward Pitch

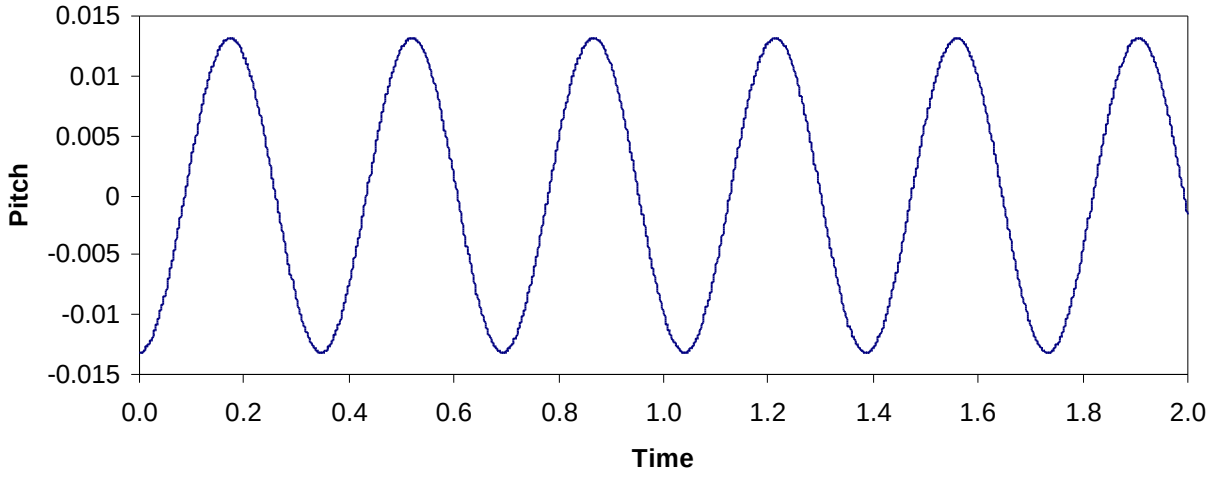

Figure 3.19. y , Undamped Free Vibration, 6th Mode: Surge with Backward Pitch

3.5 Initial Large Displacements from Equilibrium

The modes of vibration that have been determined are only valid for small motions about equilibrium. In section 3.4, these modes were verified with the nonlinear equations when imposing small displacements on the breakwater and then allowing the structure to vibrate. However, since this is a nonlinear analysis, it is important to know which DOFs are coupled together for large motions as well. This can be determined on a case by case basis for each DOF by initially displacing the cylinder by a large amount in only one DOF and leaving all the others at their equilibrium values. The six nonlinear EOMs, Equations 2.46-2.51, are then evaluated by substituting in these values. If any of the six acceleration terms in these equations is a nonzero number, then that DOF is coupled with the DOF in question. A FORTRAN program was written to conduct this evaluation and the results showed that the same terms that were coupled together in the linear free vibration analysis remained coupled except that heave was added to each relationship. In other words, the nonlinear coupled terms are: surge, pitch, and heave; sway, roll, and heave; yaw and heave; and heave only. The results of this analysis are presented in Table 3.3 and were verified with a Mathematica program.

Table 3.3. Coupled Terms For Large Motions

Initial Displacements (All other DOFs at equil.)	$\ddot{x}_c$	$\ddot{y}_c$	$\ddot{z}_c$	$\ddot{\psi}$	$\ddot{\theta}$	$\ddot{\phi}$
$x_{c\_o} = 1.0$	-49.2	-5.05	0	61.6	0	0
$y_{c\_o} = 1.0$	0	-123	0	0	0	0
$z_{c\_o} = 1.0$	0	-5.05	-49.2	0	0	-134
$\psi_o = 1.0$	140	-212	0	-207	0	0
$\theta_o = 1.0$	0	-162	0	0	-278	0
$\phi_o = 1.0$	0	-50.4	-60.0	0	0	-130

3.5.1 Transition from Small to Large Displacements

To display the difference between the linear and nonlinear EOMs, the transition from small motions to large motions is represented in the time histories in Figures 3.20-3.31. The graphs are all free vibration time histories starting in the first mode, with the initial conditions incrementally increasing for each graph. The ratio of the eigenvector for the first mode is maintained between the initial translations and rotations for each plot. At slightly higher initial conditions than Figures 3.10 and 3.11, the curves in Figures 3.20 and 3.21 are very similar except that they are not as smooth. Small vibrations appear to begin forming at the peaks. In addition, Figure 3.21 shows that small heave motions begin to develop, where before there was no heave vibration. Figures 3.23-3.28 show the continuation in theses developments, while the motions remain periodic. However, the period of motion grows as the initial displacements increase, further showing that the free vibration behavior leaves the linear modes of vibration. Furthermore, small high frequency vibrations slowly develop along the path of the vibrations as the initial conditions increase. These intermediate vibrations are larger at the peaks of the surge and pitch curves. Similarly, for heave, the motion is periodic with small high frequency

vibrations; however, the small vibrations develop quicker than in surge and pitch. They do not initiate at the peaks like the other two DOFs. The period for heave also increases with higher initial displacements.

For a large initial displacement, the free vibration behavior becomes completely different than that for small and medium-sized initial displacements. Figures 3.29-3.31 show that when starting the cylinder at a surge value equivalent to the radius of the cylinder and initially rotating it at 13.4^{o} in pitch, the breakwater does not vibrate about its equilibrium positions for surge, pitch, and heave. Rather, the original equilibrium states for the three DOFs have become unstable. None of the responses are truly periodic, but the behaviors do seem to repeat to an extent.

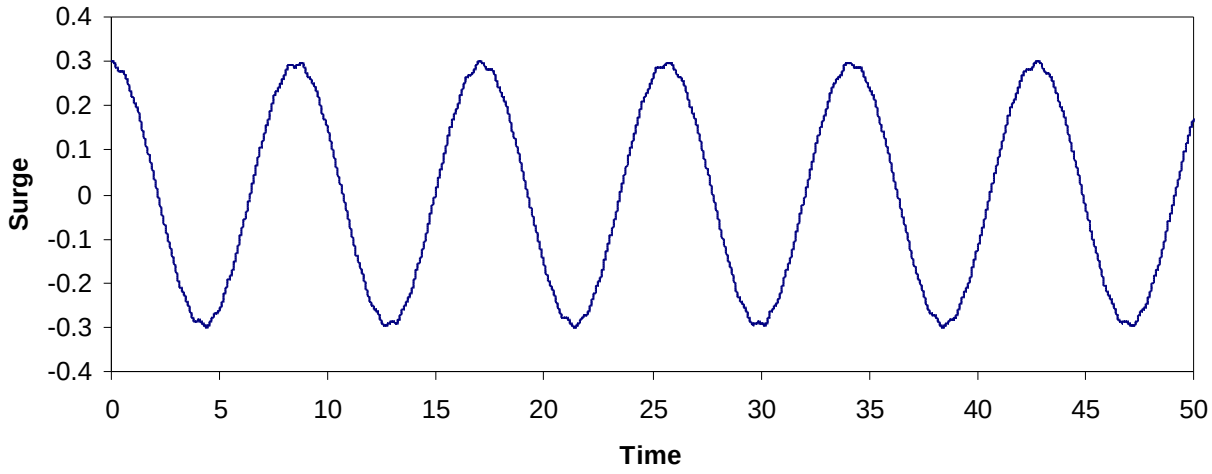

Figure 3.20. x_c, 1st Mode: Surge with Forward Pitch, $x_{c\_o} = 0.3$

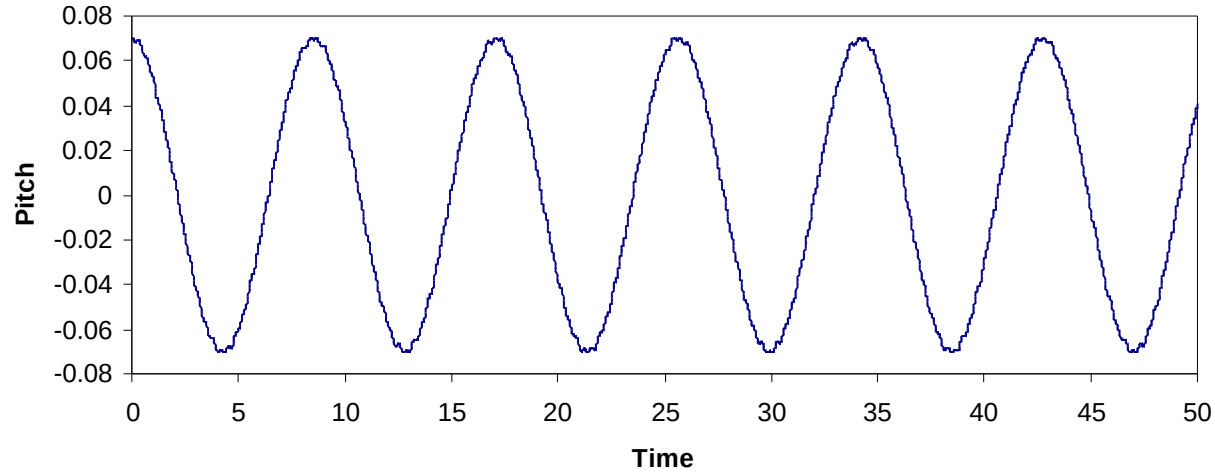

Figure 3.21. y , 1st Mode: Surge with Forward Pitch, $y_o = 0.0702$

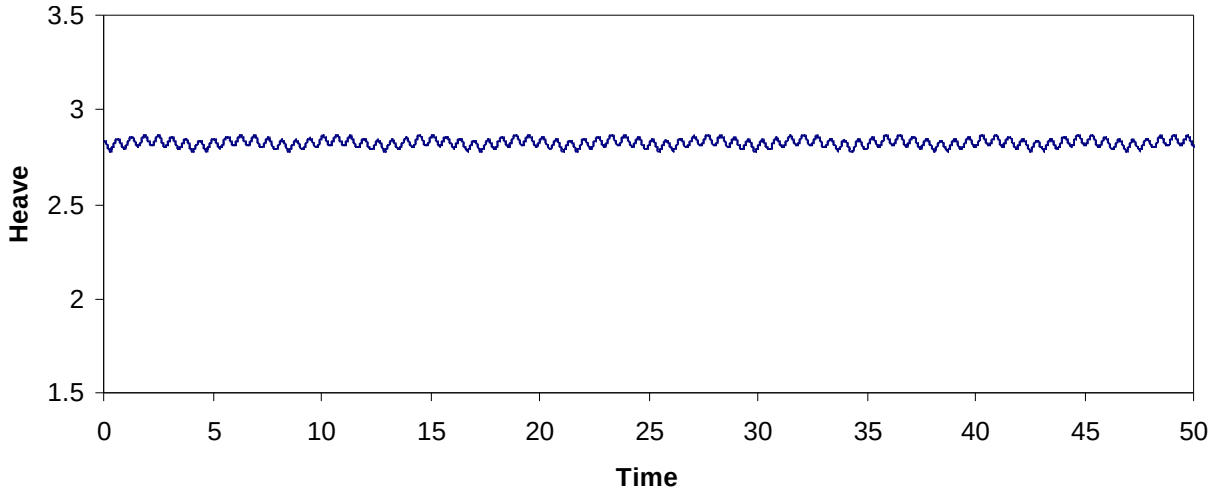

Figure 3.22. y_c, 1st Mode: Surge with Forward Pitch, $y_{c\_o} = y_{c\_eq}$

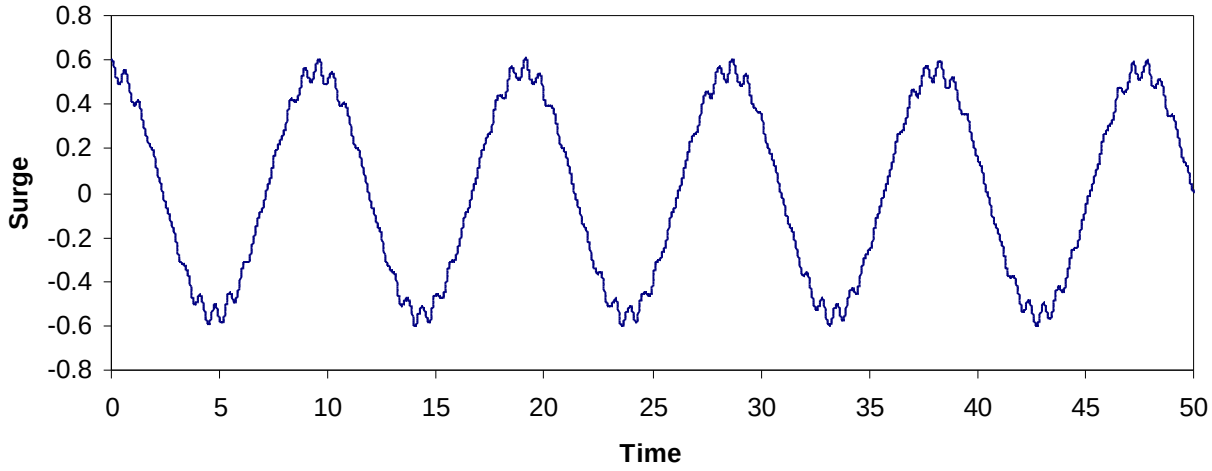

Figure 3.23. x_c, 1st Mode: Surge with Forward Pitch, $x_{c\_o} = 0.6$

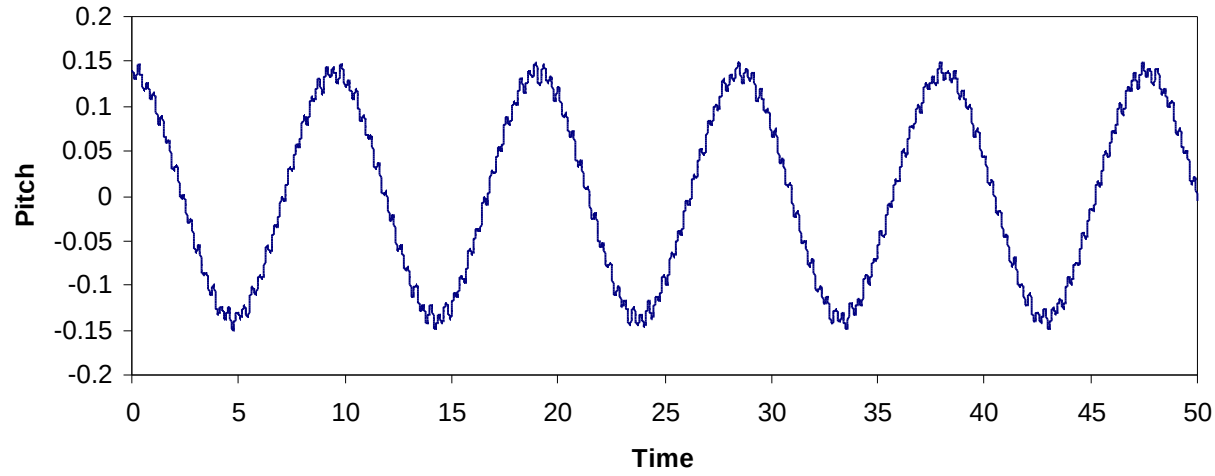

Figure 3.24. y , 1st Mode: Surge with Forward Pitch, $y_{c\_o} = 0.1404$

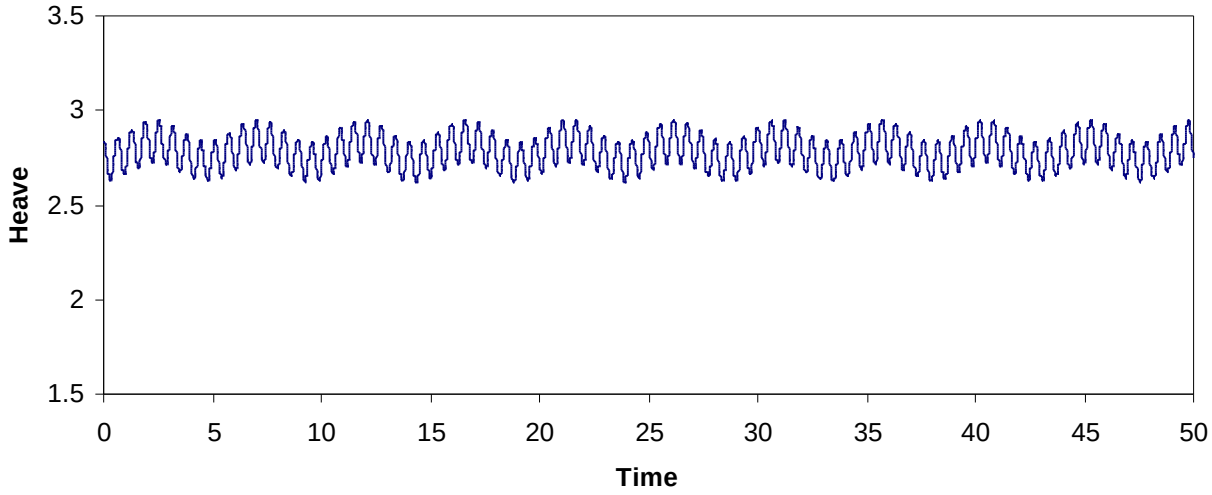

Figure 3.25. y_c, 1st Mode: Surge with Forward Pitch, $y_{c\_o} = y_{c\_eq}$

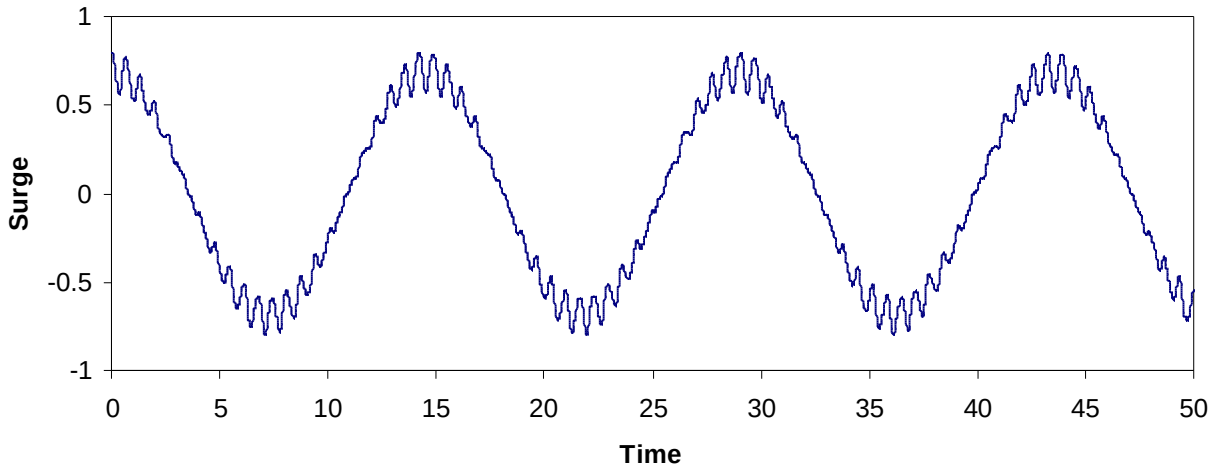

Figure 3.26. x_c, 1st Mode: Surge with Forward Pitch, $x_{c\_o} = 0.8$

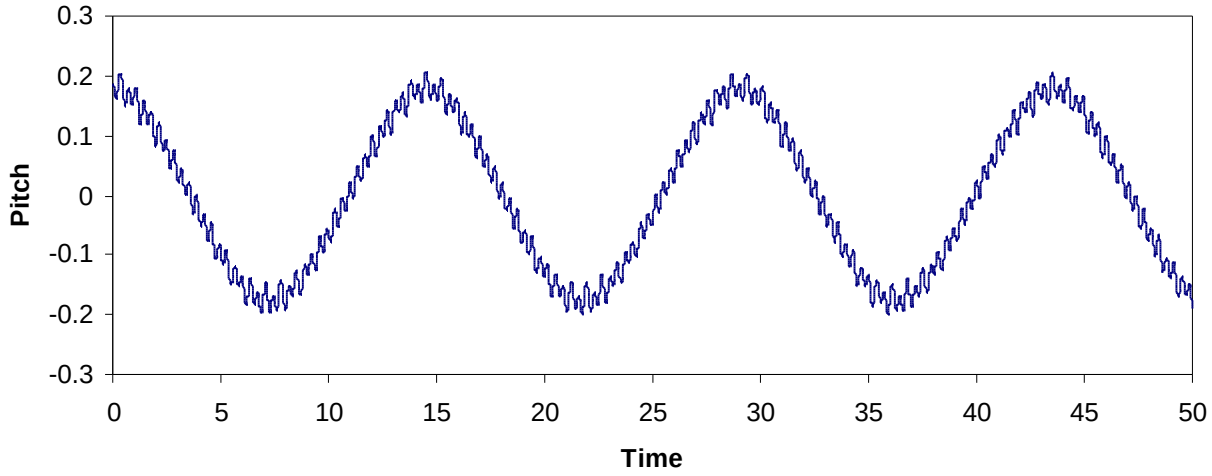

Figure 3.27. y , 1st Mode: Surge with Forward Pitch, $y_o = 0.1872$

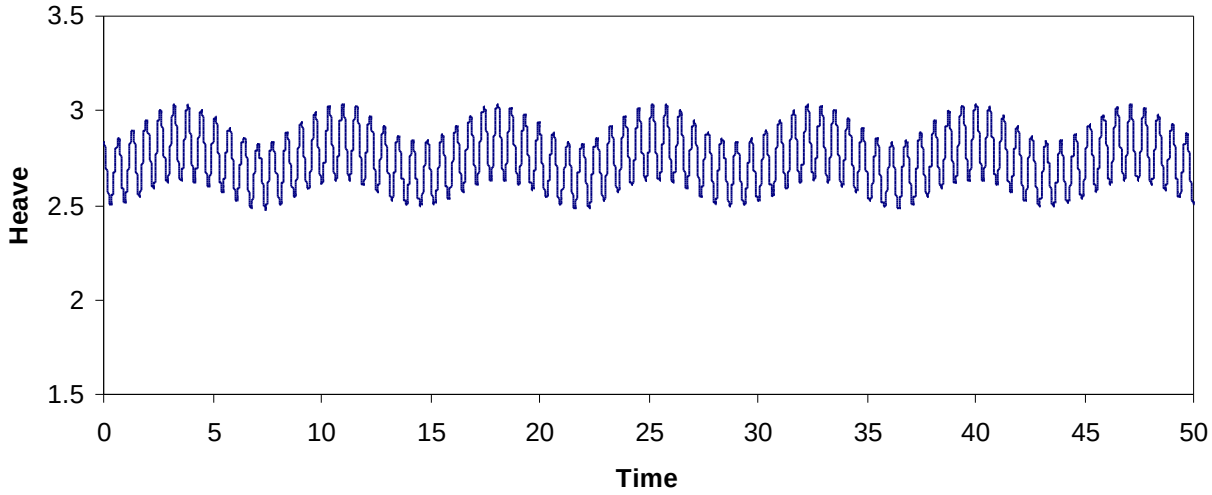

Figure 3.28. y_c, 1st Mode: Surge with Forward Pitch, $y_{c\_o} = y_{c\_eq}$

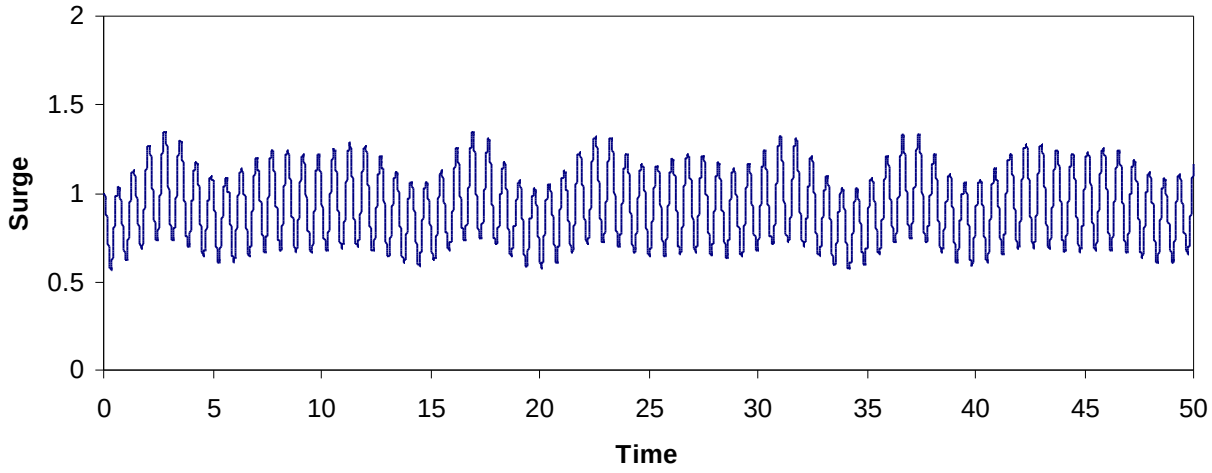

Figure 3.29. x_c, 1st Mode: Surge with Forward Pitch, x_{c_o} = 1.0

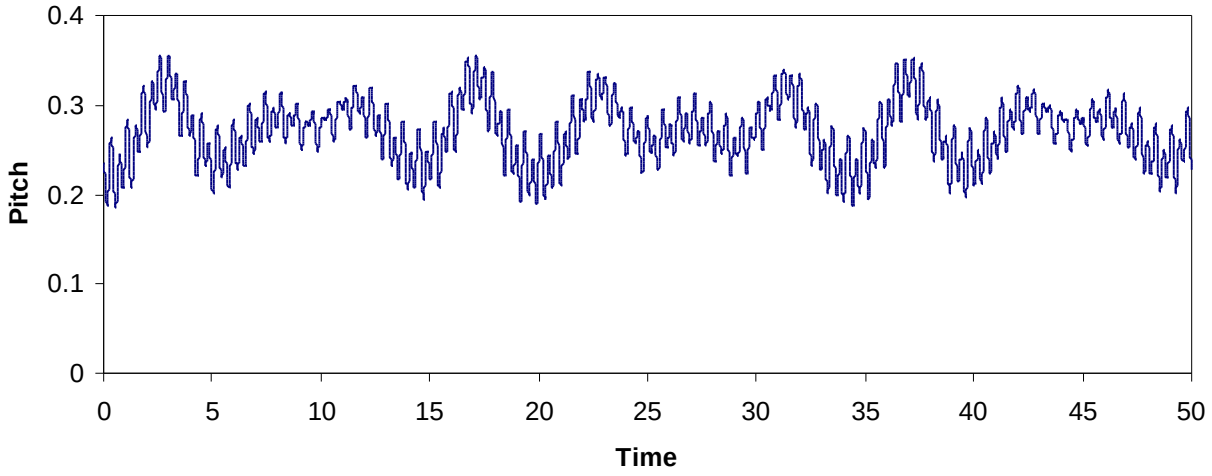

Figure 3.30. y , 1st Mode: Surge with Forward Pitch, y_o = 0.2340

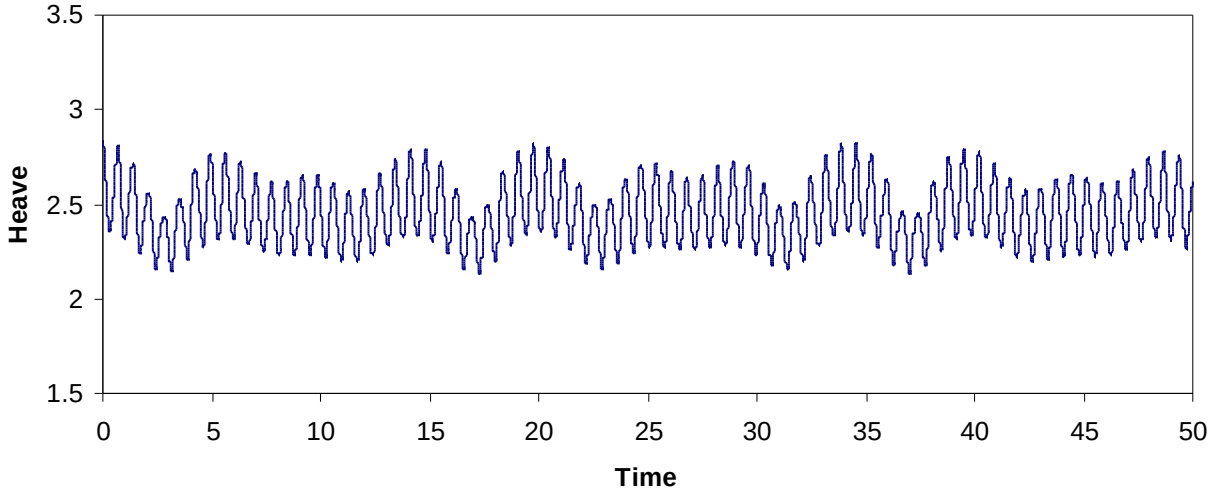

Figure 3.31. y_c, 1st Mode: Surge with Forward Pitch, $y_{c\_o} = y_{c\_eq}$

The same analysis was conducted for the breakwater's five other modes of vibration. The second mode behaves similarly to the first as the initial conditions increase, except for the two worst case scenarios, as shown in Figures 3.32-3.43. The time histories for the last two cases display a sudden change to erratic behavior, rather than a repetitive motion. In fact, the last case has displacements so large that the cylinder collapses.

The transition of the free vibration for the third mode is shown in Figures 3.44-3.51. For the first case of the third mode, the amplitude of the yaw motion appears to be slowly moving up, as shown in Figure 3.44. The motion was plotted out to $x = 50$, and the amplitude actually slowly moves back down and repeats this behavior. The first case was plotted to $x = 4$ to show that the period remains identical to that of the third mode for small motions. Figure 3.45 shows that small heave motions occur. The next case shows that the yaw motion remains at the same period, but its amplitude changes. A repeated behavior continues until about $x = 35$, when the motion shifts up. The heave motion dramatically changes and has a similar behavior repeated at a period of about 4, but it is not truly periodic. Figures 3.48-3.51 display that the last two cases show a transformation into irregular motion.

Figures 3.52-3.55 show that there is not much change in the fourth mode for large displacements when compared to small motions. The only difference is that the period of motion slightly increases from 0.63 to about 0.66 for the worst case scenario. This lack of change is due to the fact that this mode is a SDF system for the free vibration of both small and large motions.

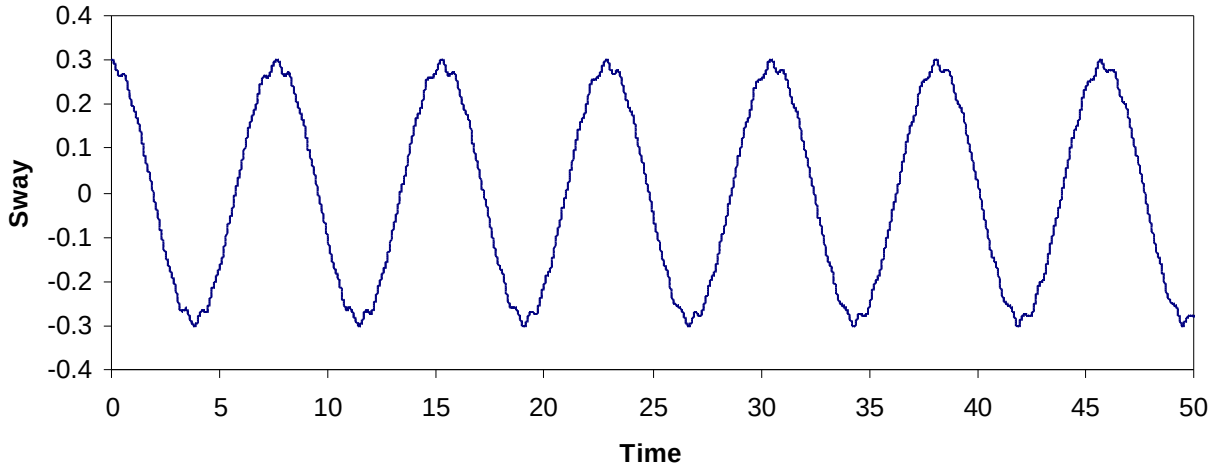

Figure 3.32. z_c, 2nd Mode: Sway with Backward Roll, z_{c_o} = 0.3

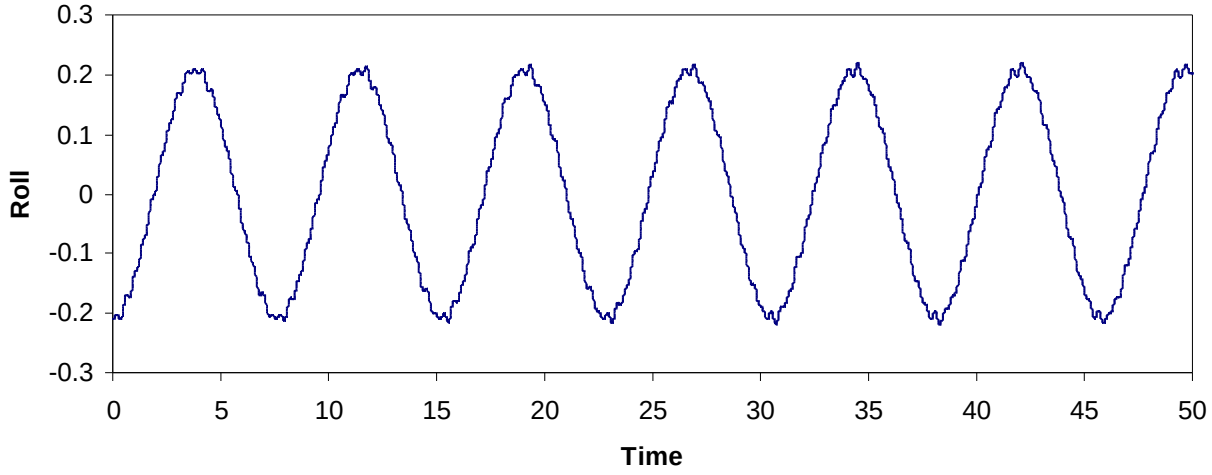

Figure 3.33. f, 2nd Mode: Sway with Backward Roll, f_o = 0.2099

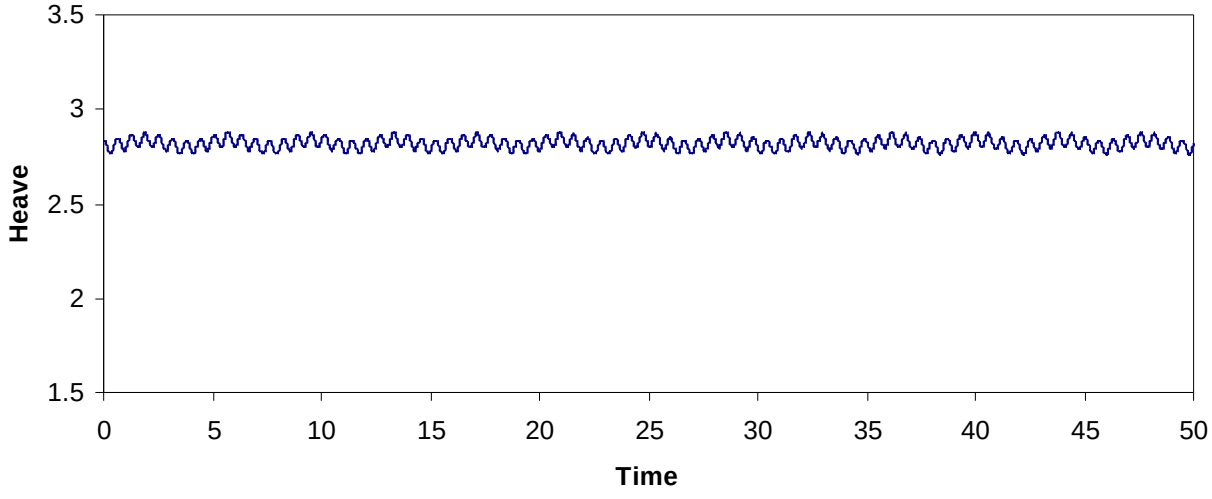

Figure 3.34. y_c, 2nd Mode: Sway with Backward Roll, $y_{c\_o} = y_{c\_eq}$

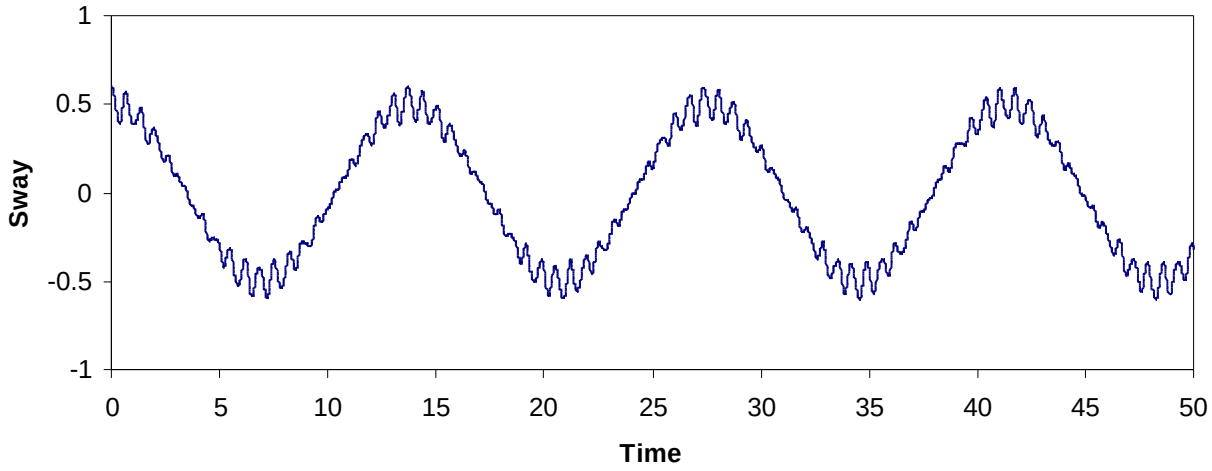

Figure 3.35. z_c, 2nd Mode: Sway with Backward Roll, z_{c_o} = 0.6

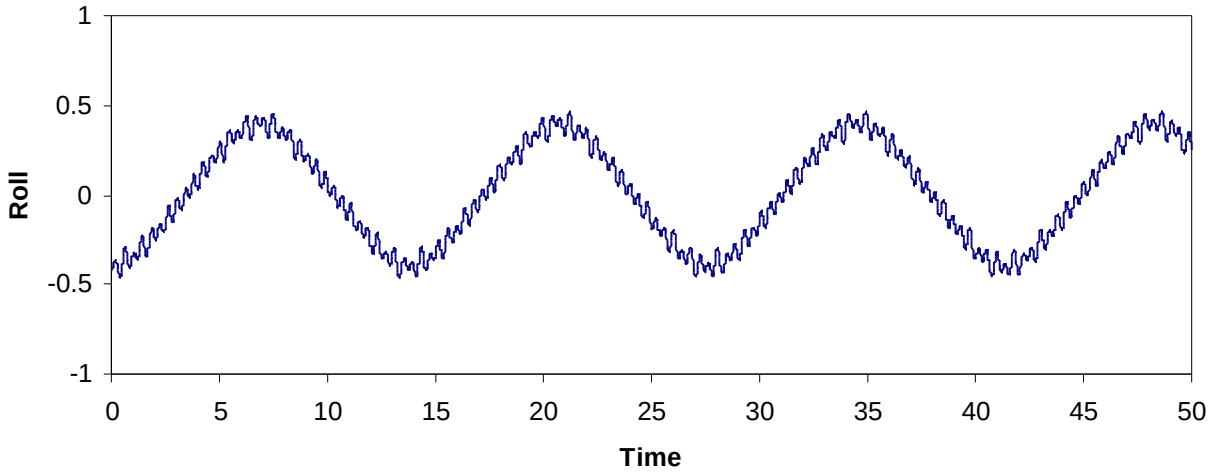

Figure 3.36. f, 2nd Mode: Sway with Backward Roll, f_o = 0.4198

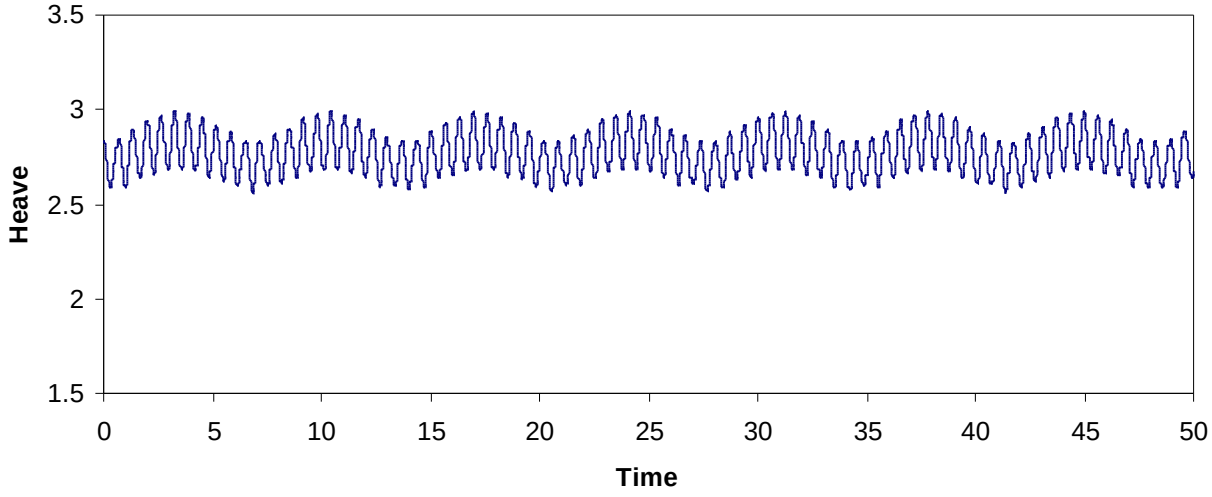

Figure 3.37. y_c, 2nd Mode: Sway with Backward Roll, $y_{c\_o} = y_{c\_eq}$

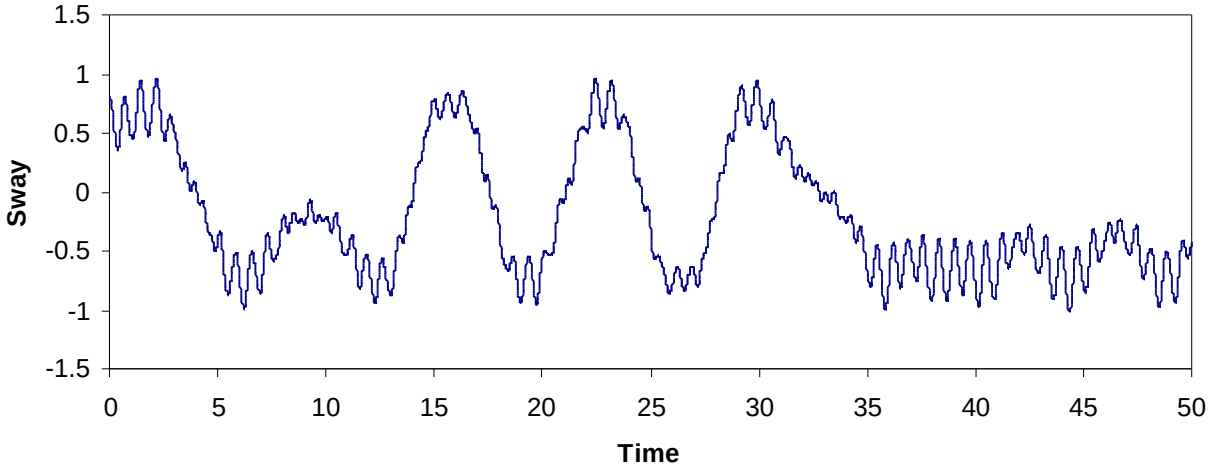

Figure 3.38. z_c, 2nd Mode: Sway with Backward Roll, z_{c_o} = 0.8

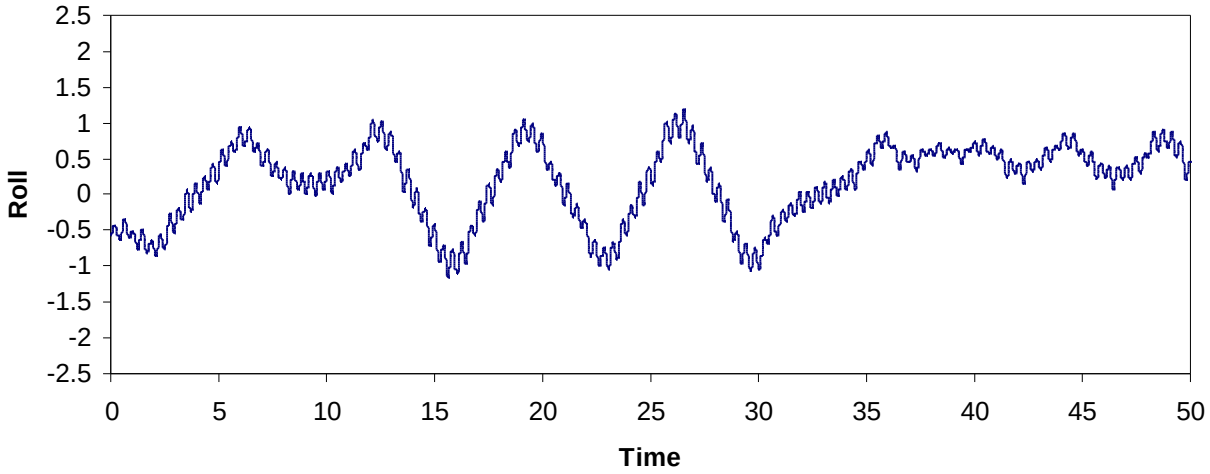

Figure 3.39. f, 2nd Mode: Sway with Backward Roll, f_o = 0.5598

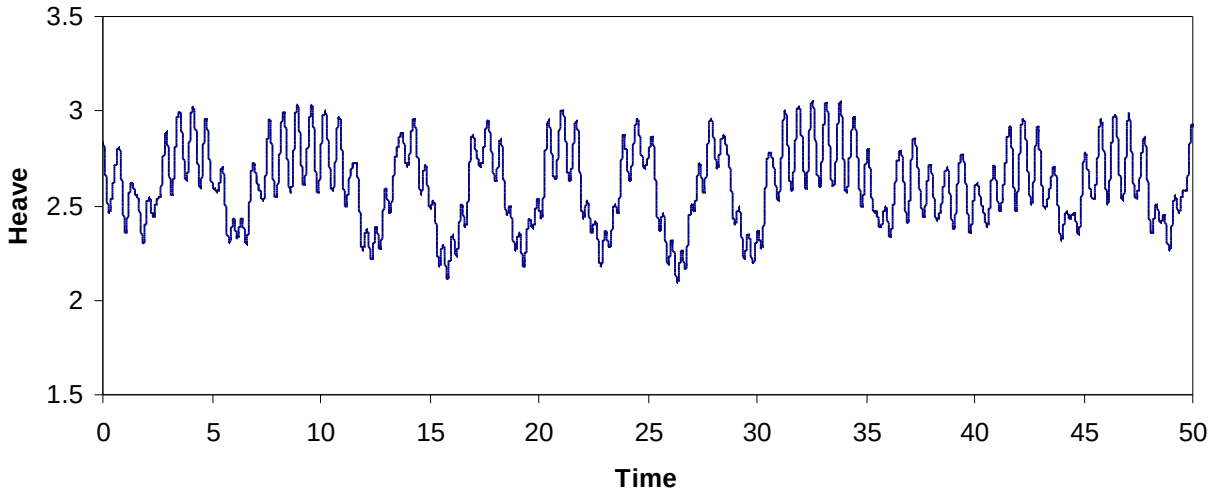

Figure 3.40. y_c, 2nd Mode: Sway with Backward Roll, $y_{c\_o} = y_{c\_eq}$

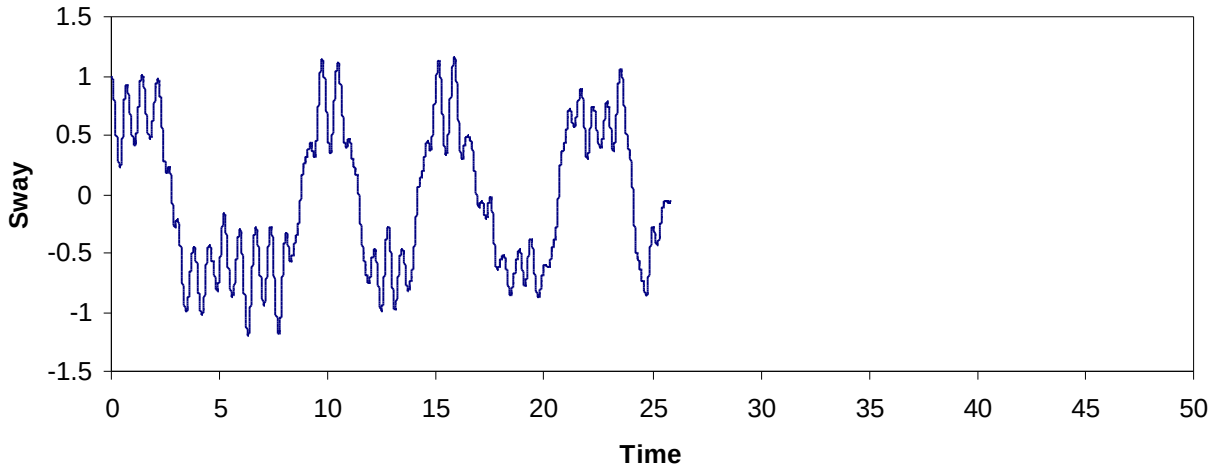

Figure 3.41. z_c, 2nd Mode: Sway with Backward Roll, z_{c_o} = 1.0

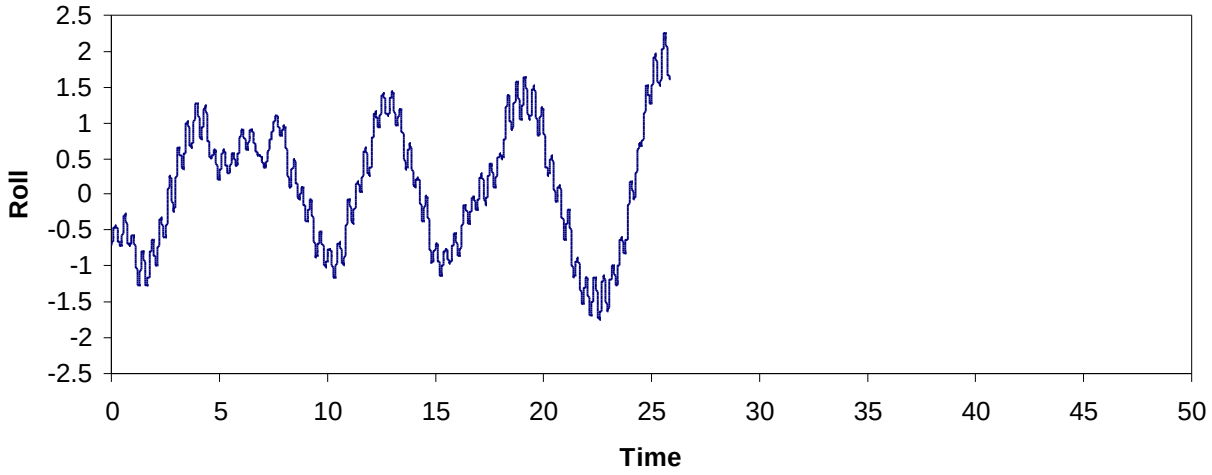

Figure 3.42. f, 2nd Mode: Sway with Backward Roll, f_o = 0.6997

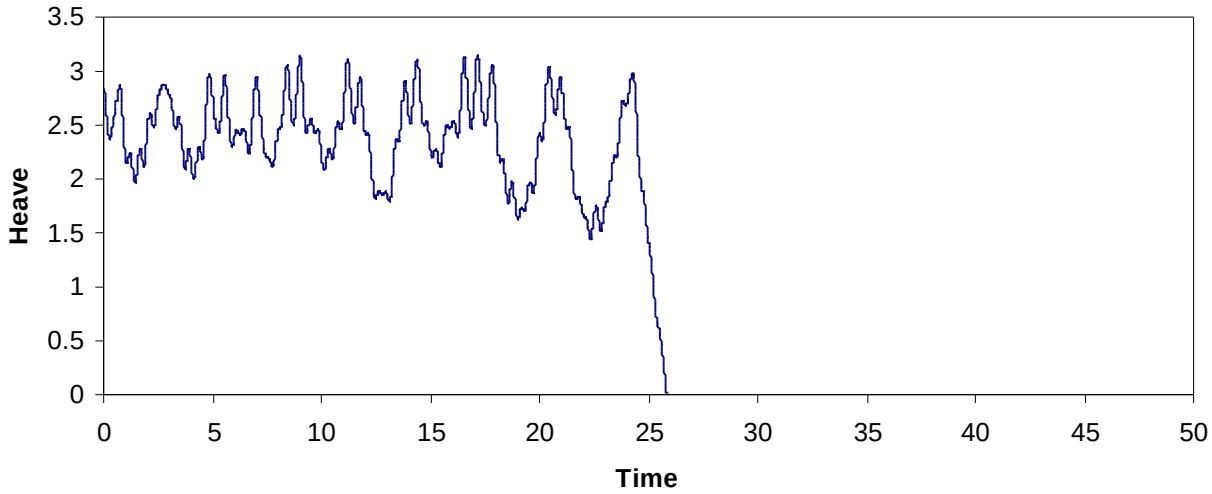

Figure 3.43. y_c, 2nd Mode: Sway with Backward Roll, $y_{c\_o} = y_{c\_eq}$

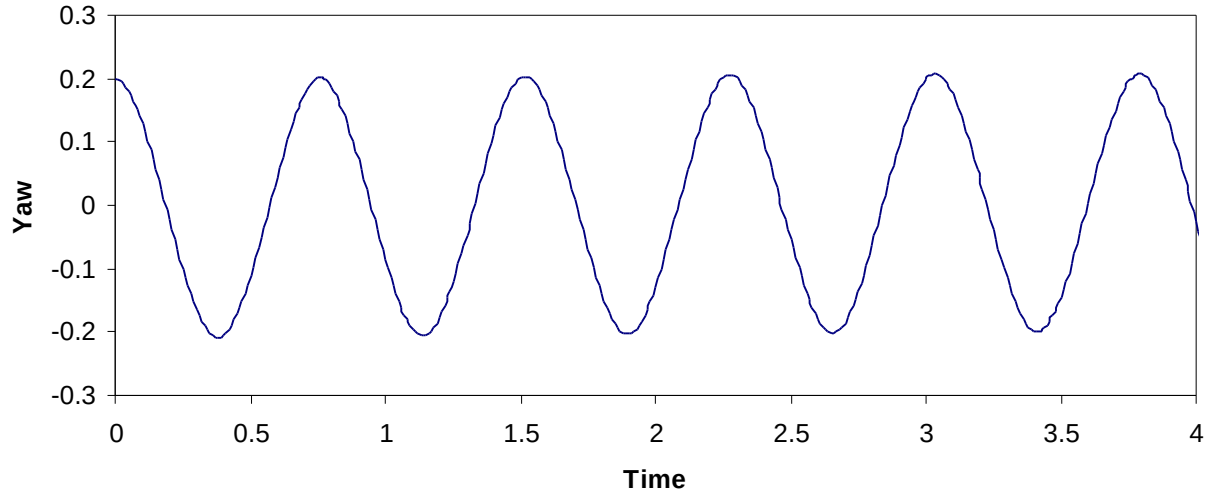

Figure 3.44. f, 3rd Mode: Yaw Only, $q_o = 0.2$

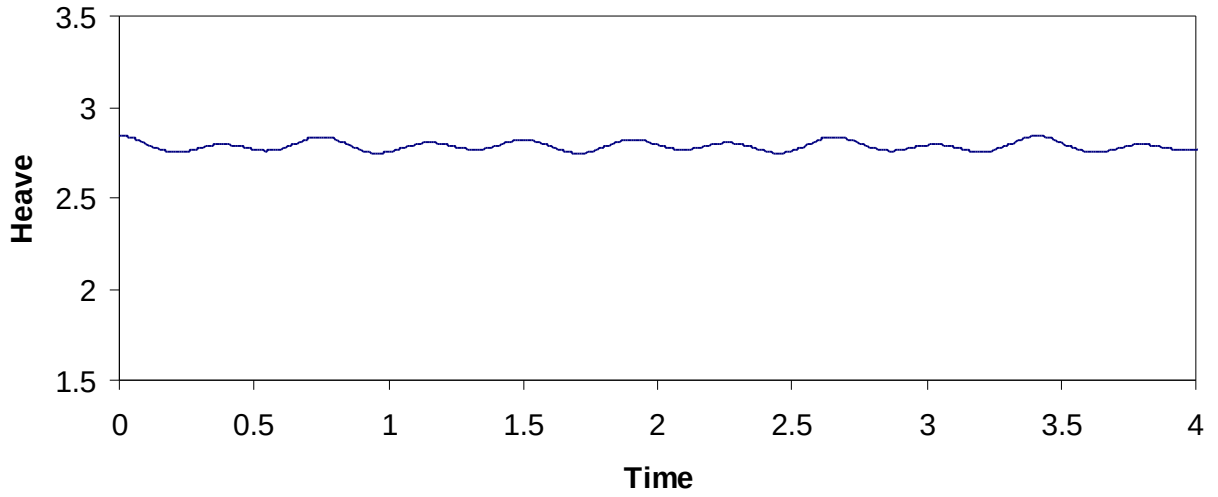

Figure 3.45. y_c, 3rd Mode: Yaw Only, $y_{c\_o} = y_{c\_eq}$

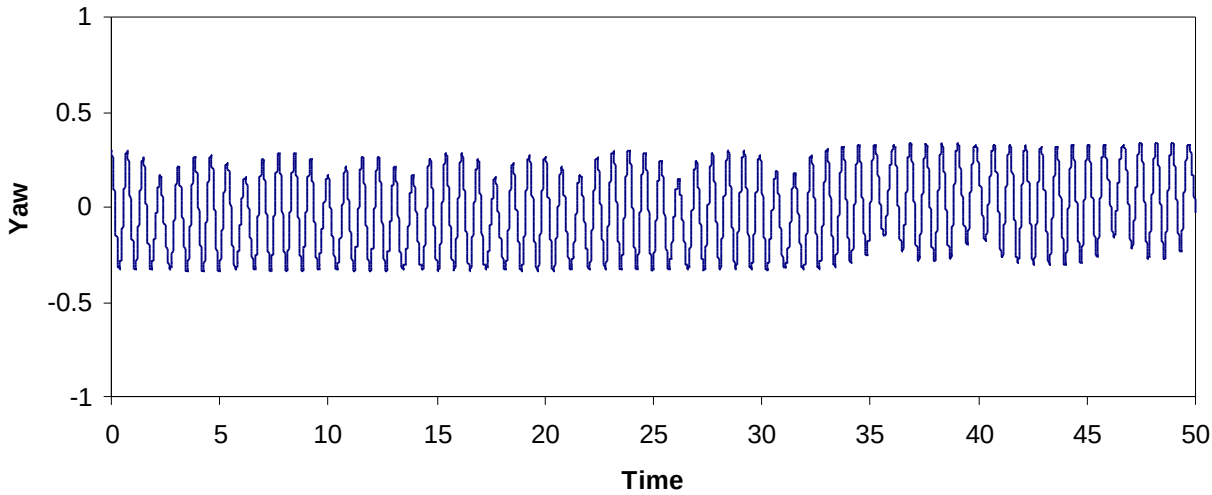

Figure 3.46. f, 3rd Mode: Yaw Only, $q_o = 0.3$

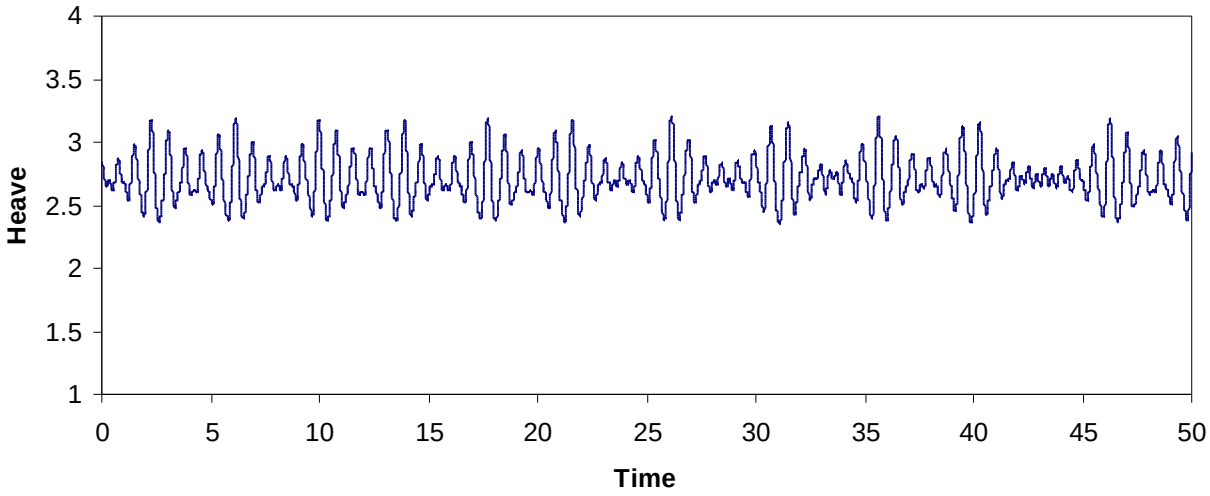

Figure 3.47. y_c, 3rd Mode: Yaw Only, $y_{c\_o} = y_{c\_eq}$

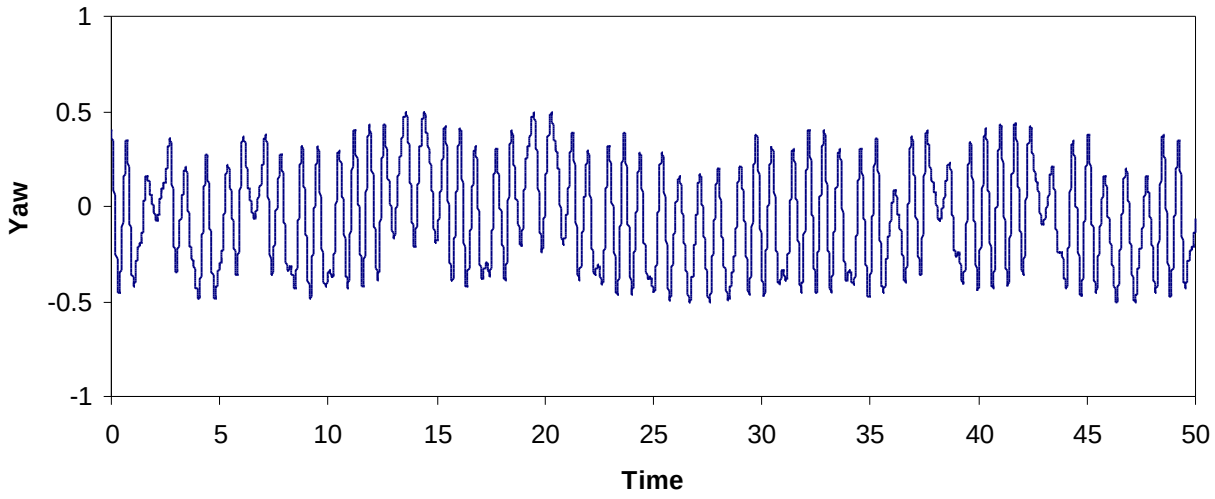

Figure 3.48. f, 3rd Mode: Yaw Only, $q_o = 0.4$

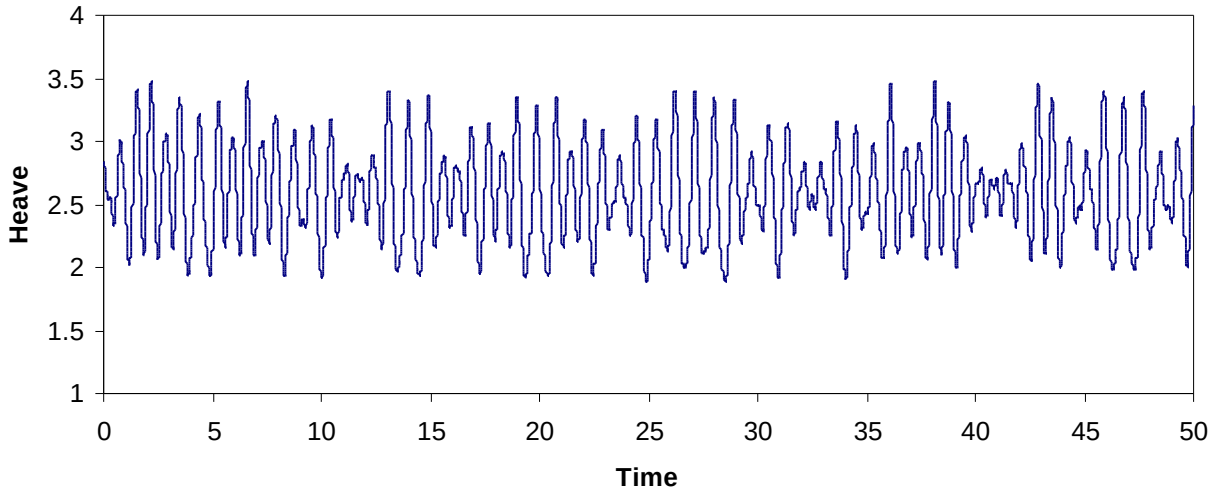

Figure 3.49. y_c, 3rd Mode: Yaw Only, $y_{c\_o} = y_{c\_eq}$

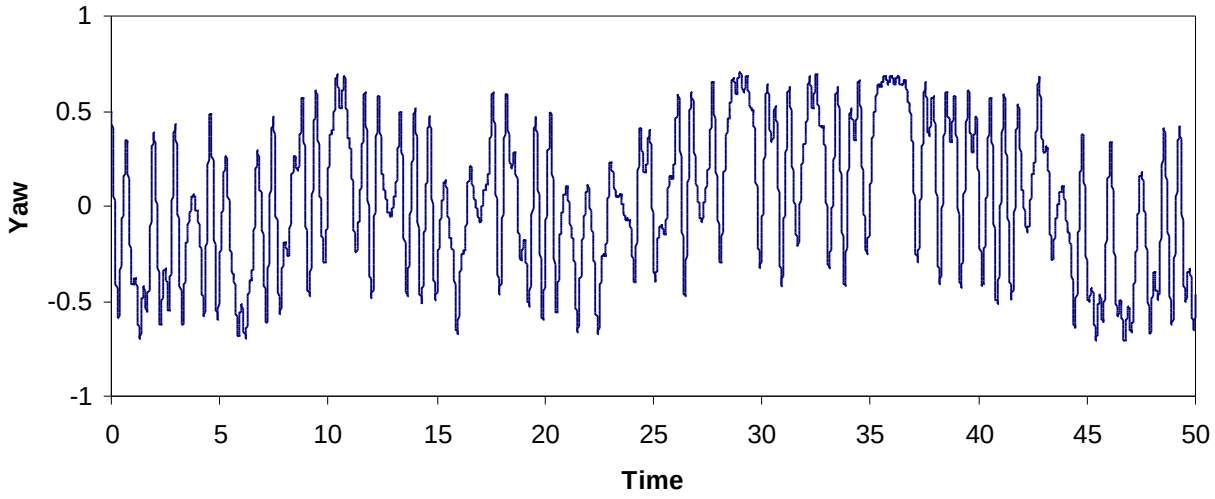

Figure 3.50. f, 3rd Mode: Yaw Only, $q_o = 0.5$

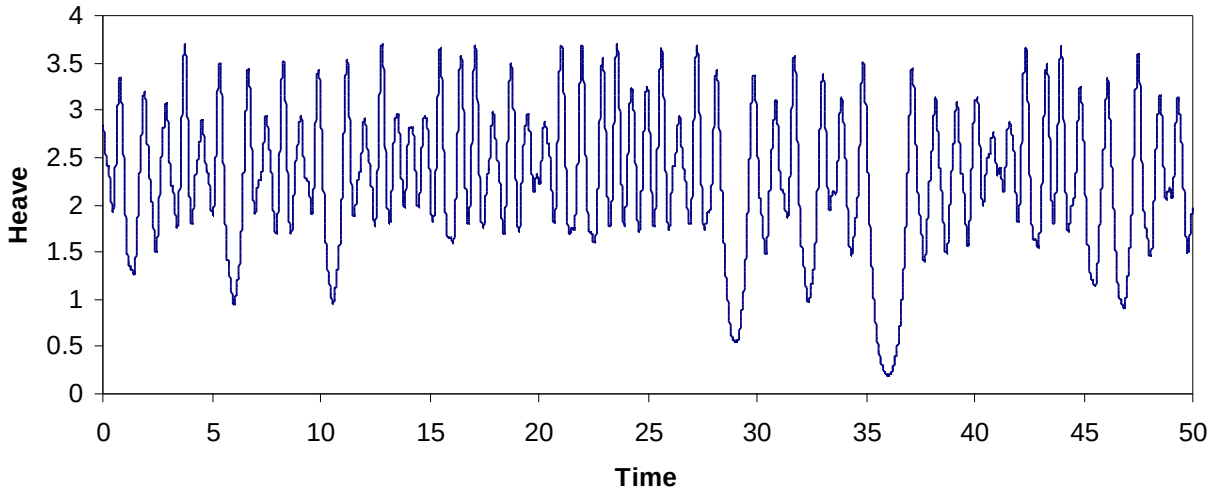

Figure 3.51. y_c, 3rd Mode: Yaw Only, $y_{c\_o} = y_{c\_eq}$

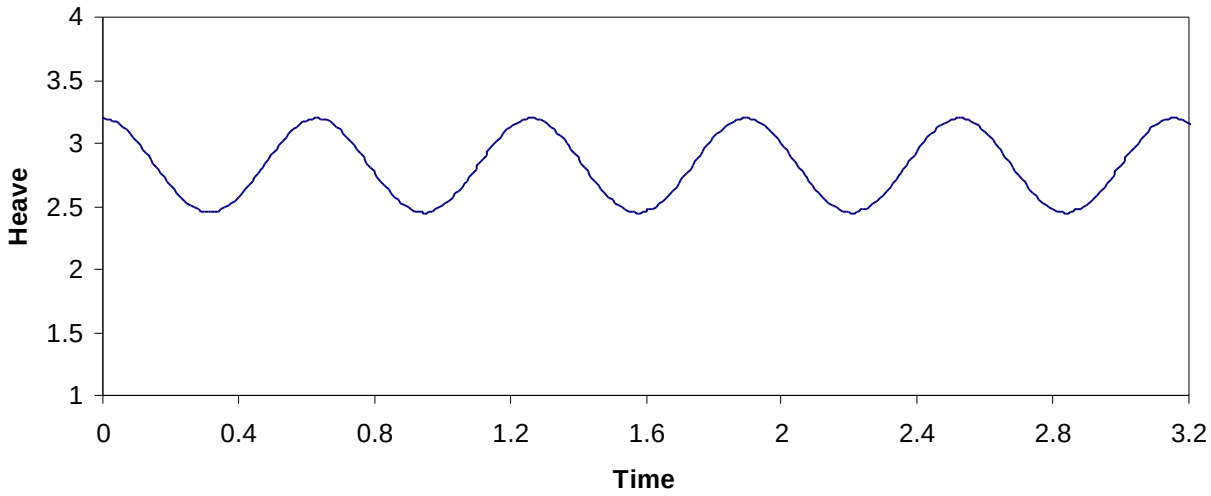

Figure 3.52. y_c, 4th Mode: Heave Only, $y_{c\_o} = 3.2$

The fifth mode does not change until the last two cases, as shown in Figures 3.56-3.66. While the period of free vibration does not change for the two worst case scenarios, the behavior dramatically transforms into quite an interesting response. The behavior in Figures 3.62-3.64 begins similarly in Figures 3.65-3.67 but at a much smaller period. Afterwards, for sway and roll, the behavior seems to continue only in the opposite direction and at a smaller period. The heave motion simply continues at a smaller period. Also, for both cases, the peaks of each DOF occur at the same times.

Figures 3.68-3.79 show that the sixth mode behaves similarly to the fifth mode. First, small wiggles begin to deform the shape of the curves as small heave motion begins to develop as well. The third case then forms odd shapes that are similar to the fifth mode and the peaks for the three DOFs occur at the same times for this mode as well. The last case starts with shapes similar to the third case, but eventually shifts up and becomes more erratic.

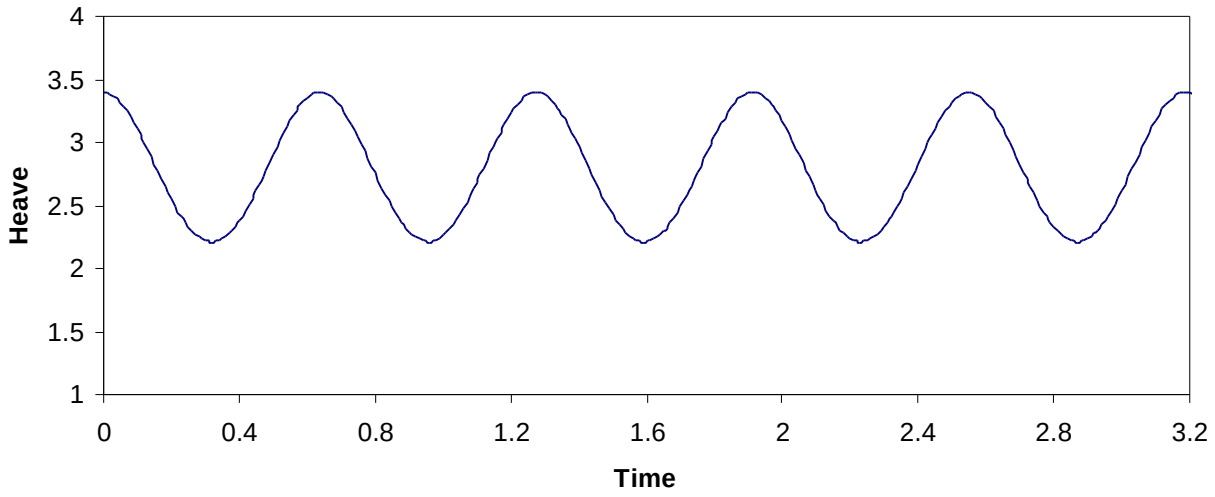

Figure 3.53. y_c, 4th Mode: Heave Only, y_{c_o} = 3.4

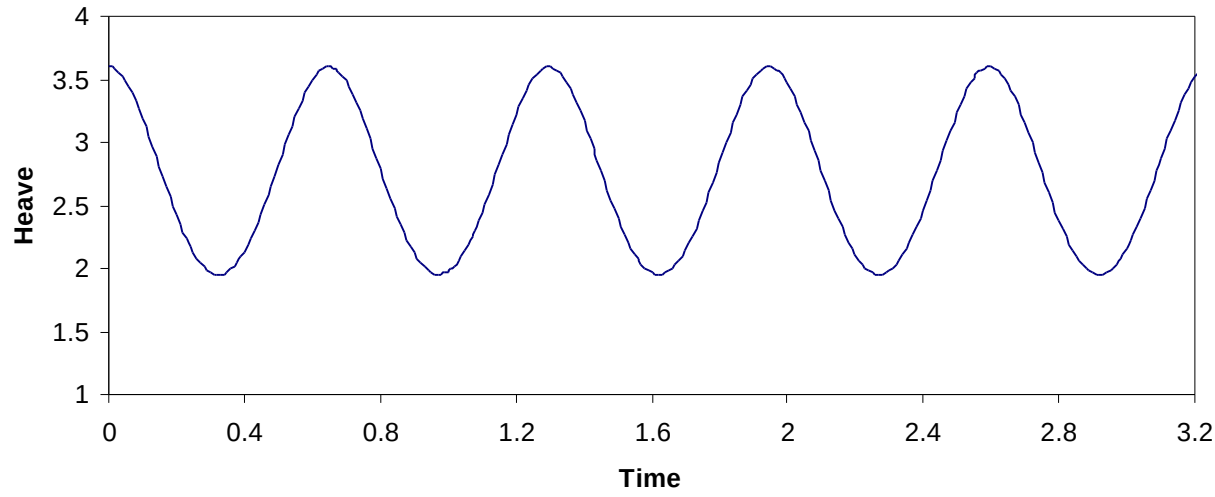

Figure 3.54. y_c, 4th Mode: Heave Only, y_{c_o} = 3.6

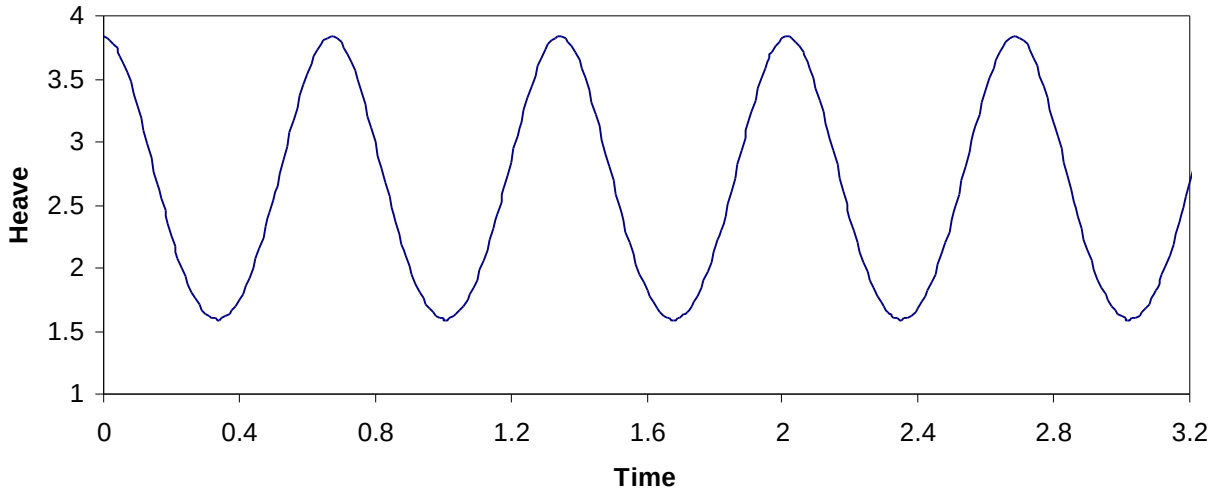

Figure 3.55. y_c, 4th Mode: Heave Only, $y_{c\_o} = y_{c\_eq} + 1$

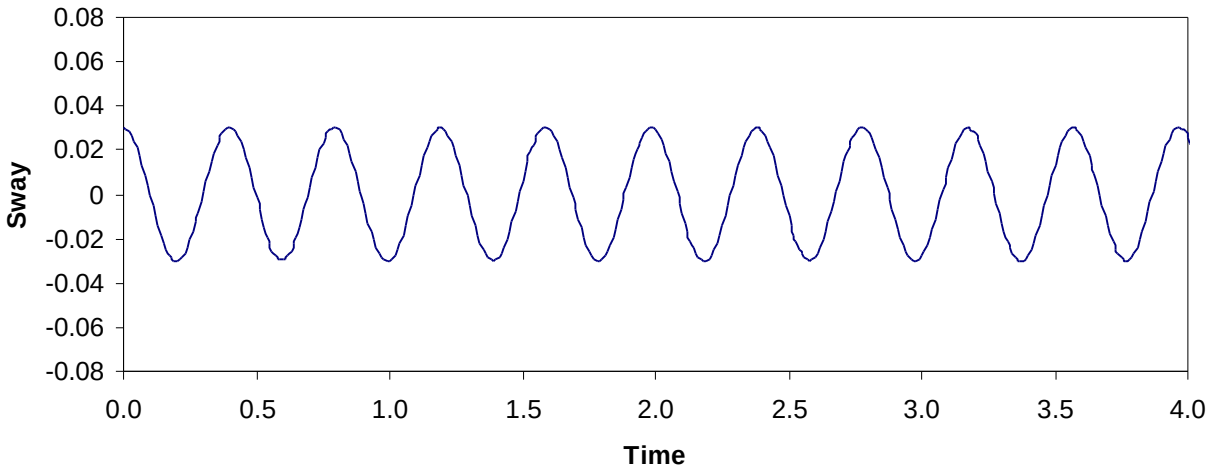

Figure 3.56. z_c, 5th Mode: Sway with Forward Roll, z_{c_o} = 0.03

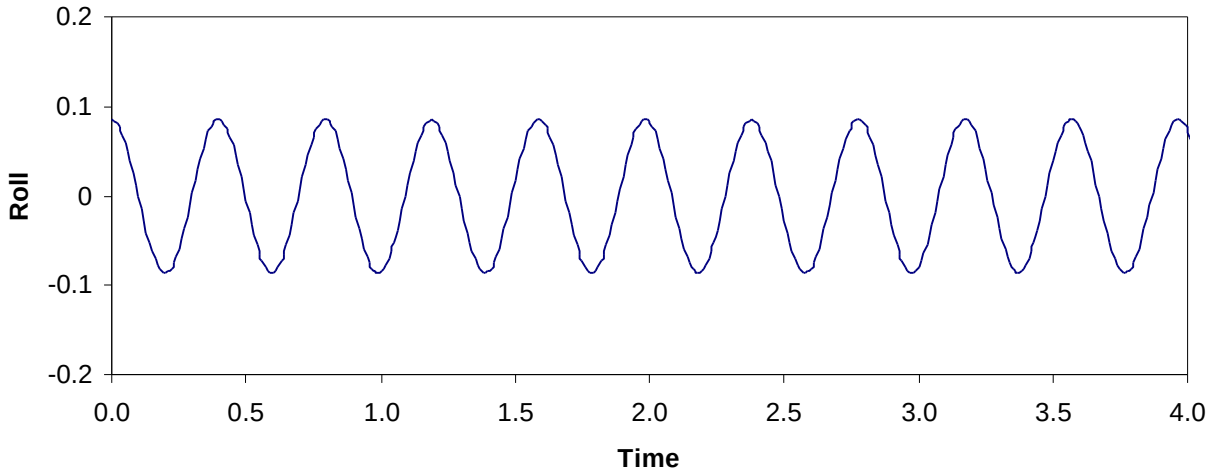

Figure 3.57. f_c, 5th Mode: Sway with Forward Roll, f_o = 0.0857

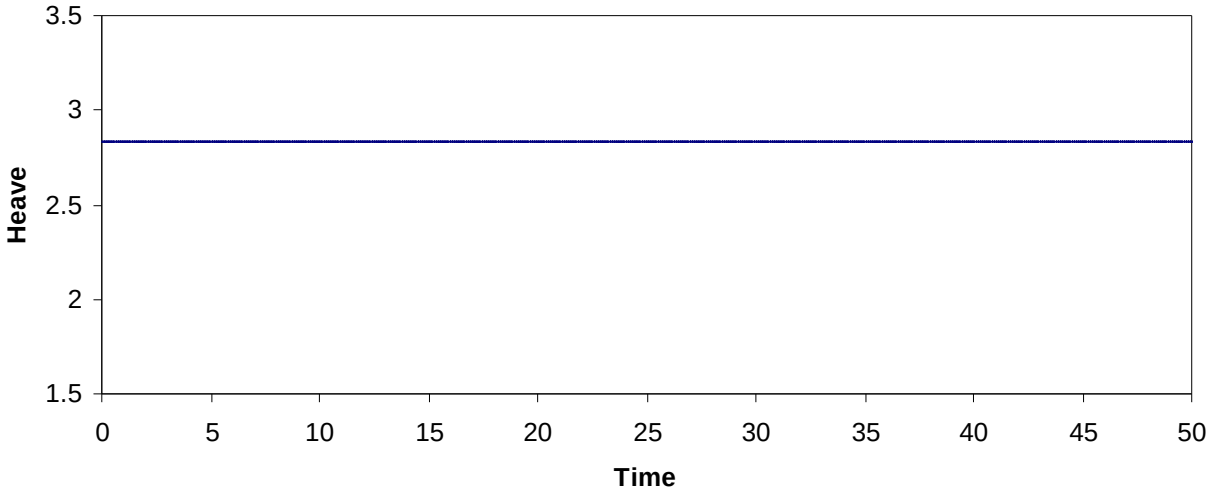

Figure 3.58. y_c, 5th Mode: Sway with Forward Roll, $y_{c\_o} = y_{c\_eq}$

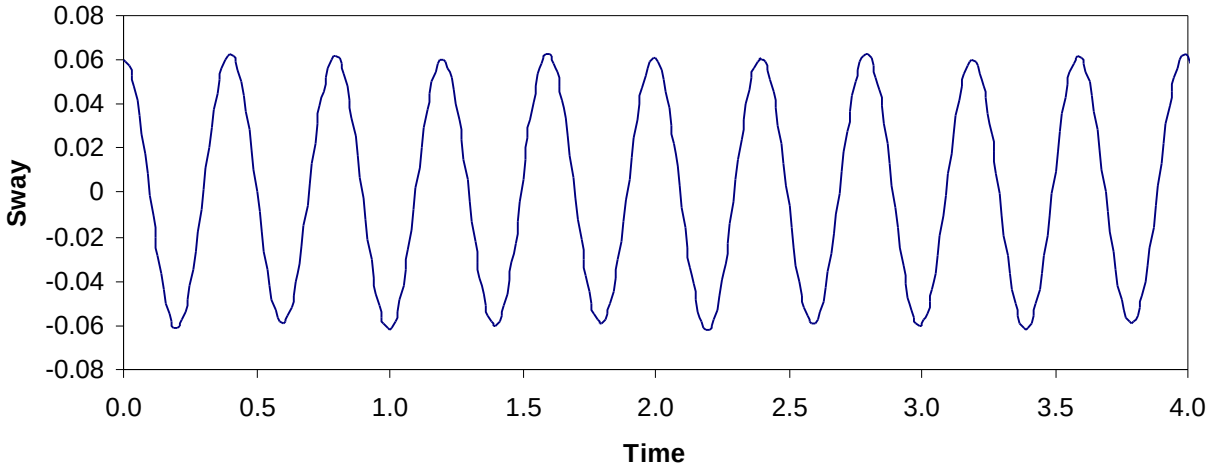

Figure 3.59. z_c, 5th Mode: Sway with Forward Roll, z_{c_o} = 0.06

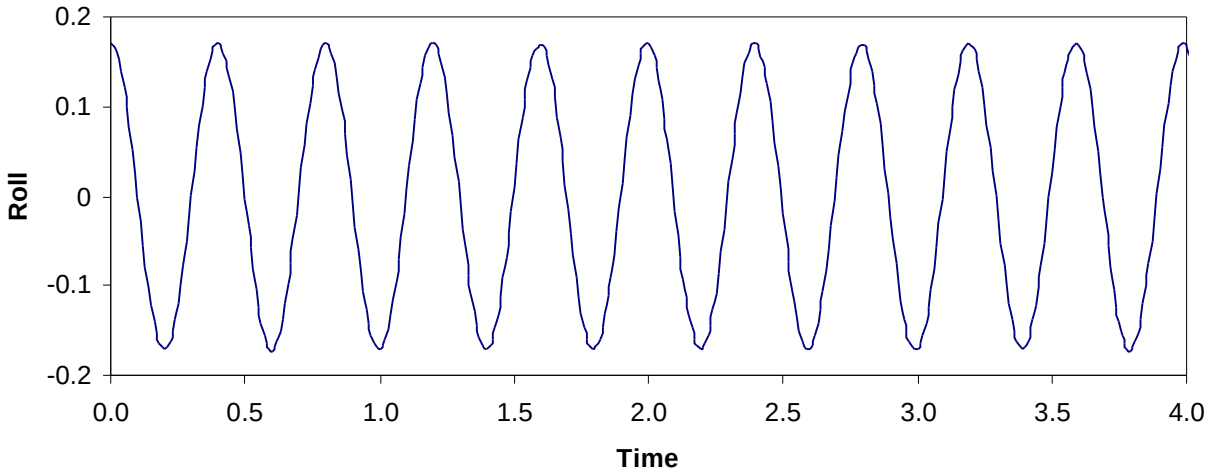

Figure 3.60. f, 5th Mode: Sway with Forward Roll, f_o = 0.1715

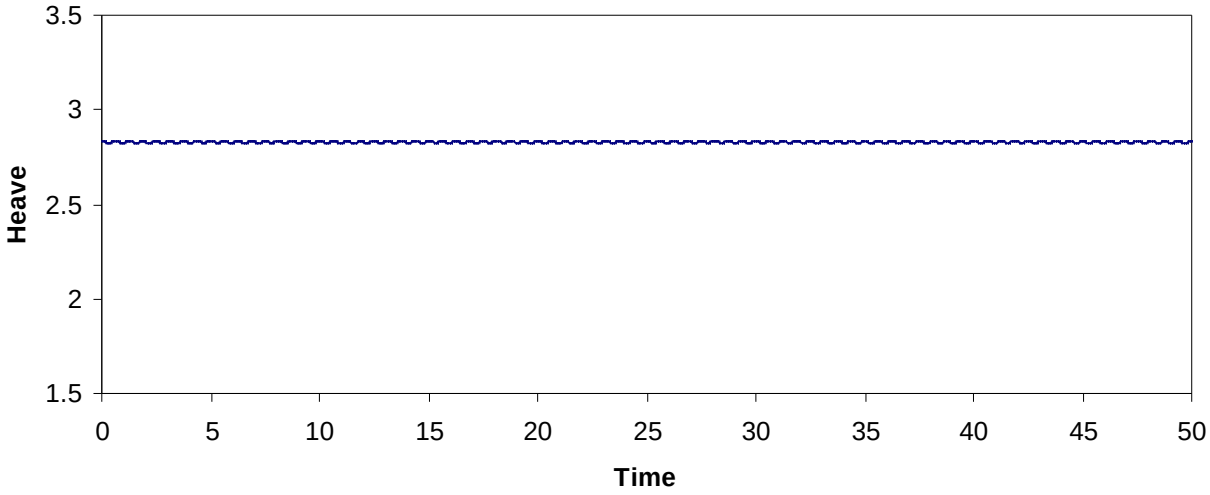

Figure 3.61. y_c, 5th Mode: Sway with Forward Roll, $y_{c\_o} = y_{c\_eq}$

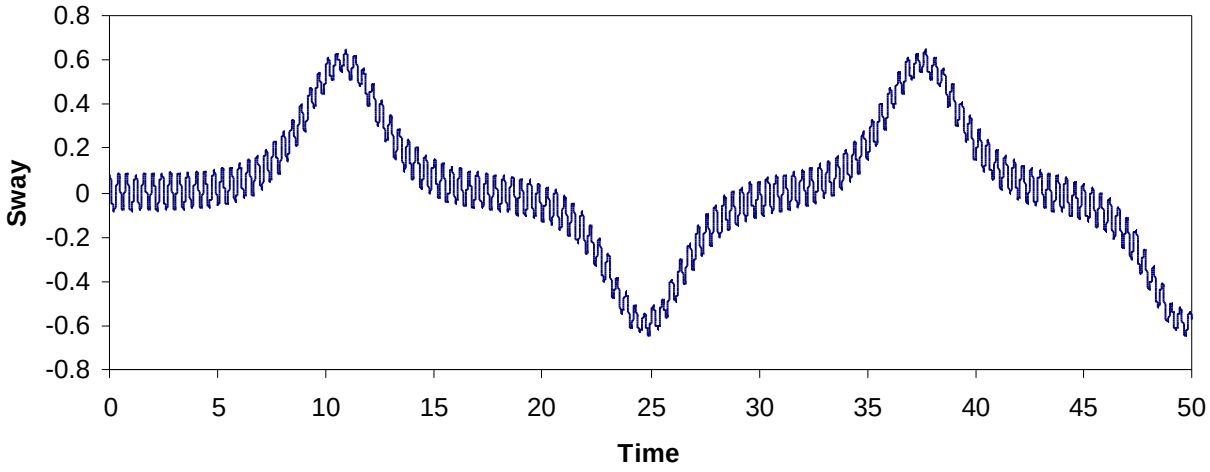

Figure 3.62. z_c, 5th Mode: Sway with Forward Roll, z_{c_o} = 0.08

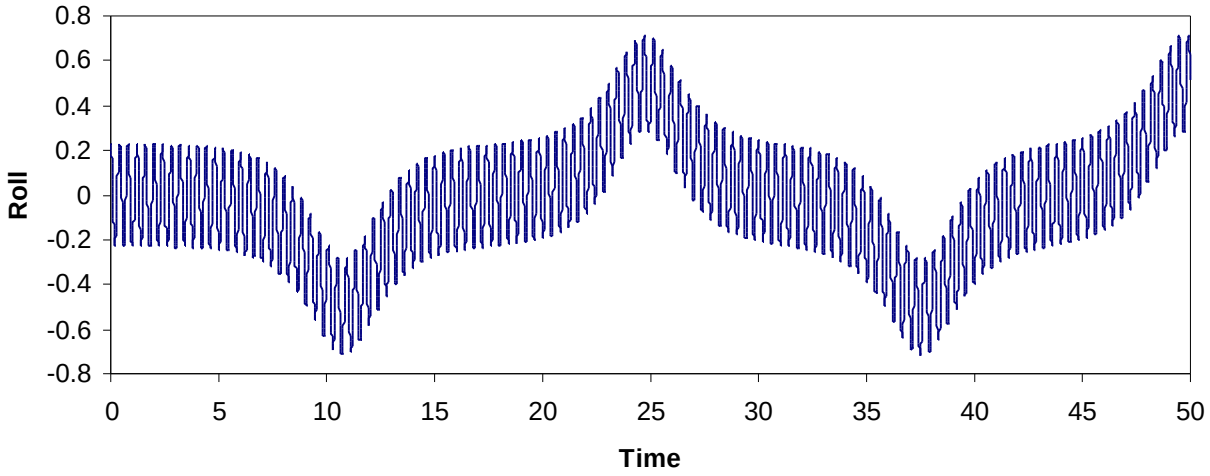

Figure 3.63. f, 5th Mode: Sway with Forward Roll, f_o = 0.2287

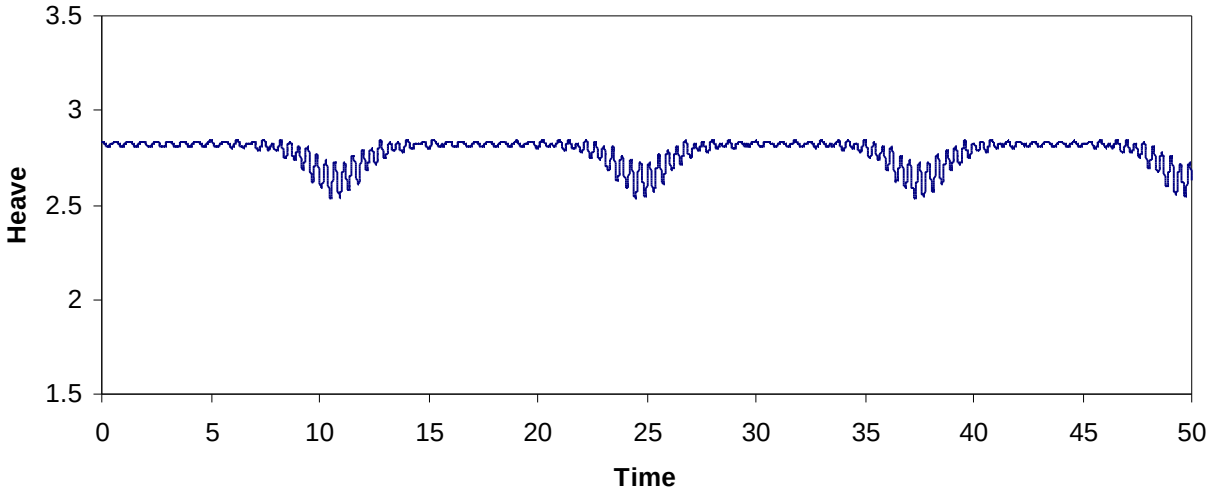

Figure 3.64. y_c, 5th Mode: Sway with Forward Roll, $y_{c\_o} = y_{c\_eq}$

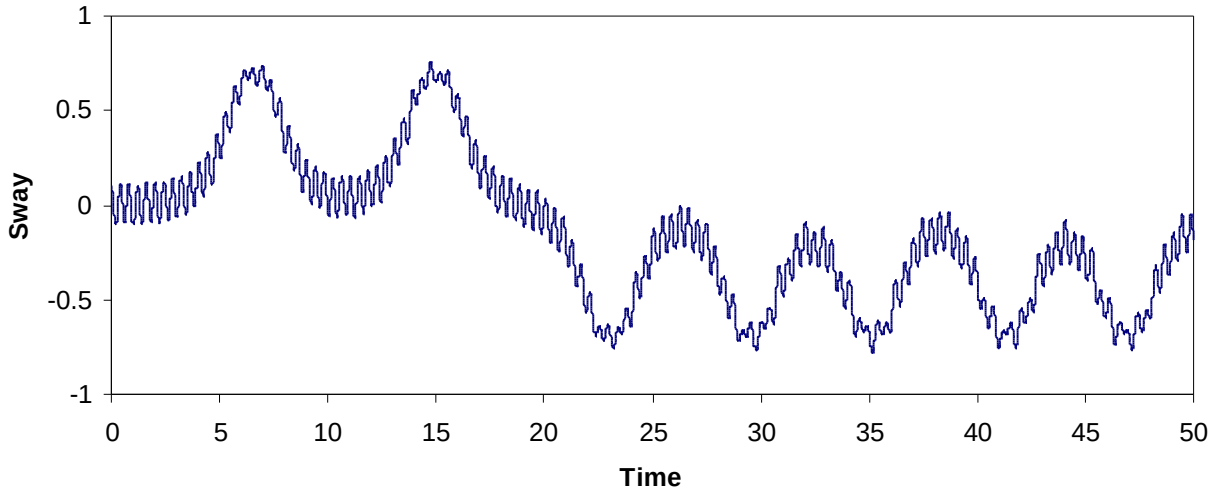

Figure 3.65. z_c, 5th Mode: Sway with Forward Roll, z_{c_o} = 0.1

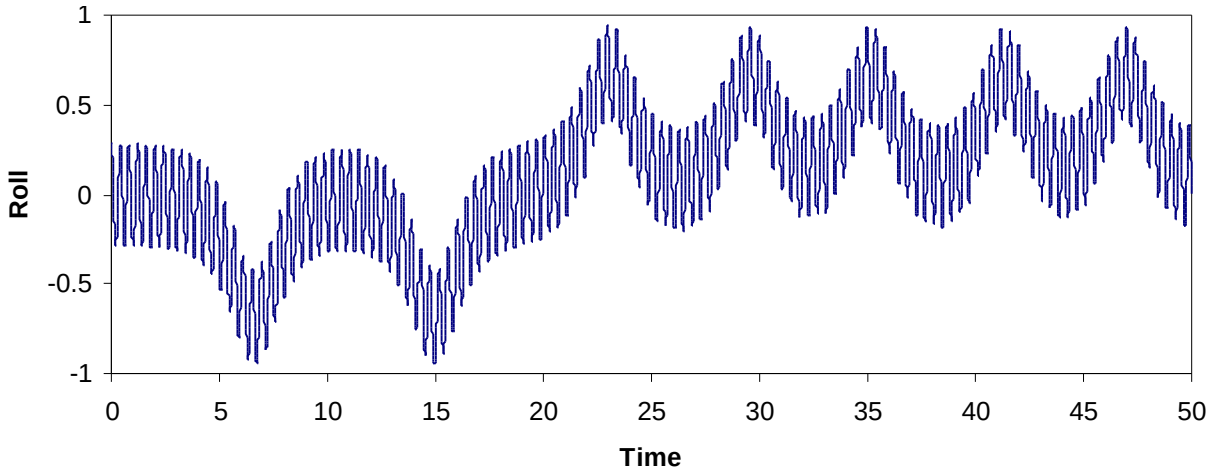

Figure 3.66. f, 5th Mode: Sway with Forward Roll, f_o = 0.2858

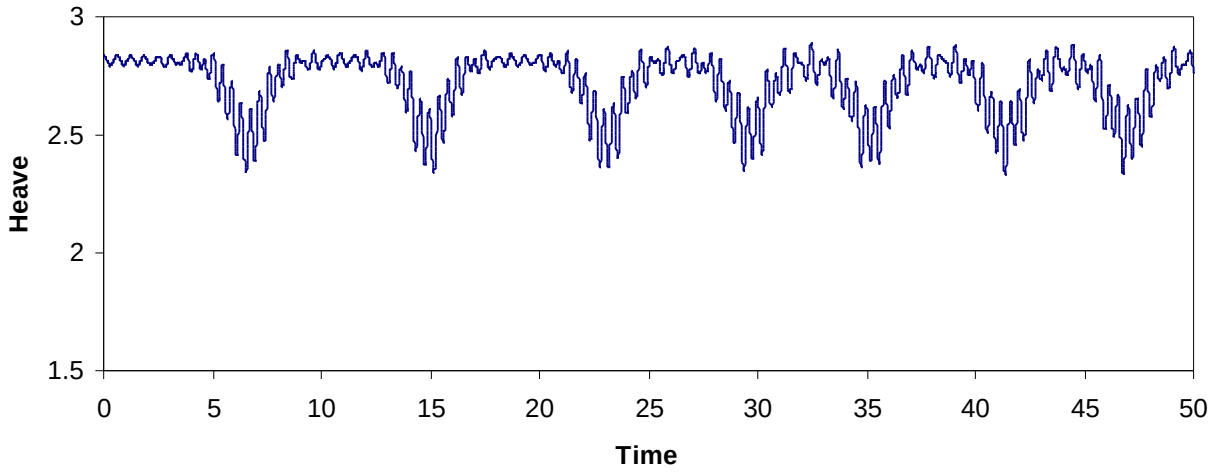

Figure 3.67. y_c, 5th Mode: Sway with Forward Roll, $y_{c\_o} = y_{c\_eq}$

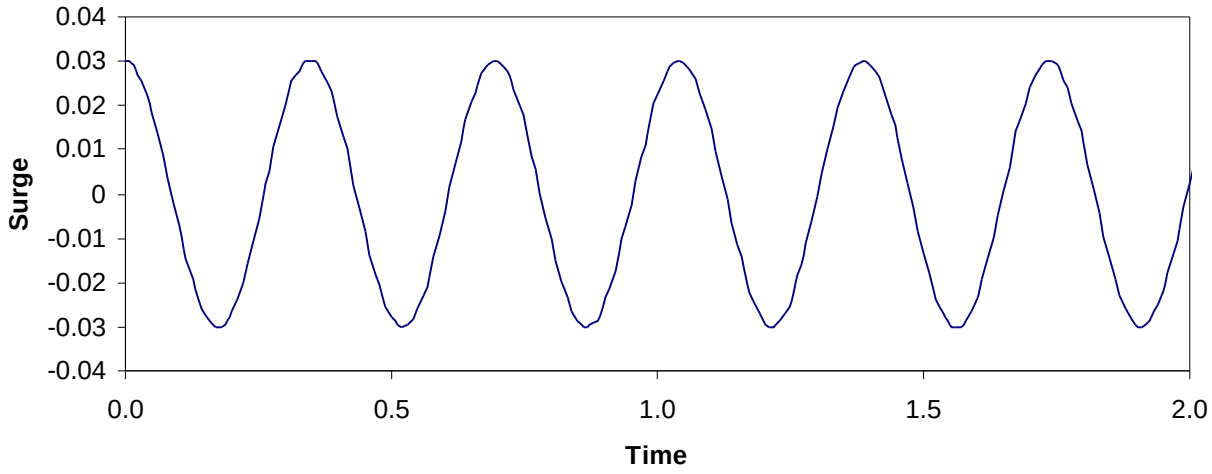

Figure 3.68. x_c, 1st Mode: Surge with Backward Pitch, x_{c_o} = 0.03

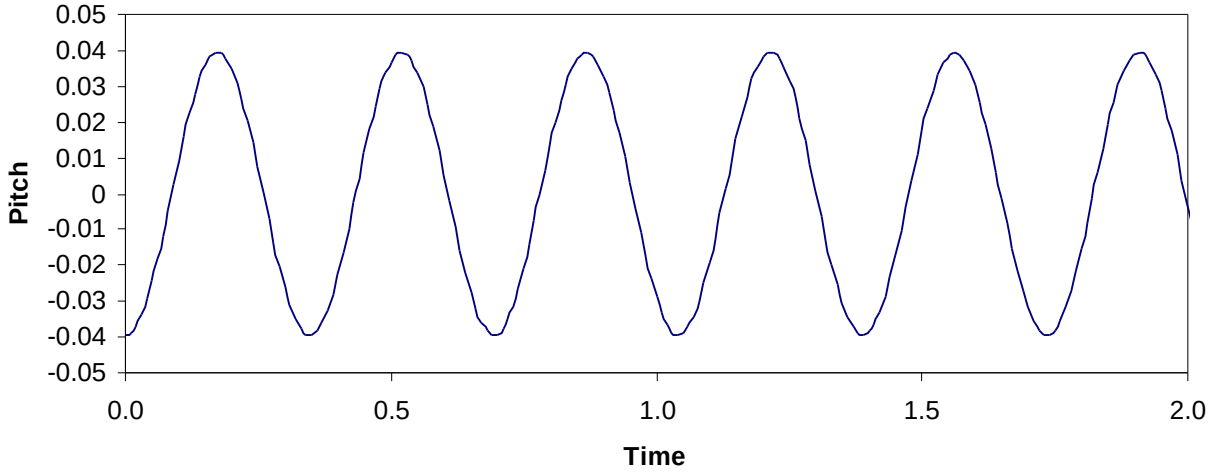

Figure 3.69. y , 1st Mode: Surge with Backward Pitch, y_o = -0.0395

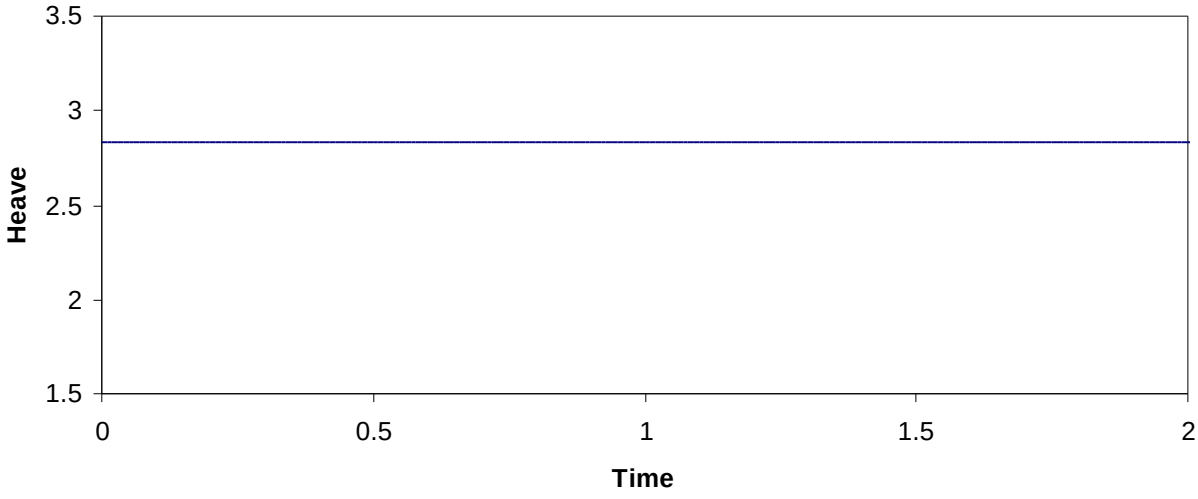

Figure 3.70. y_c, 6th Mode: Surge with Backward Pitch, $y_{c\_o} = y_{c\_eq}$

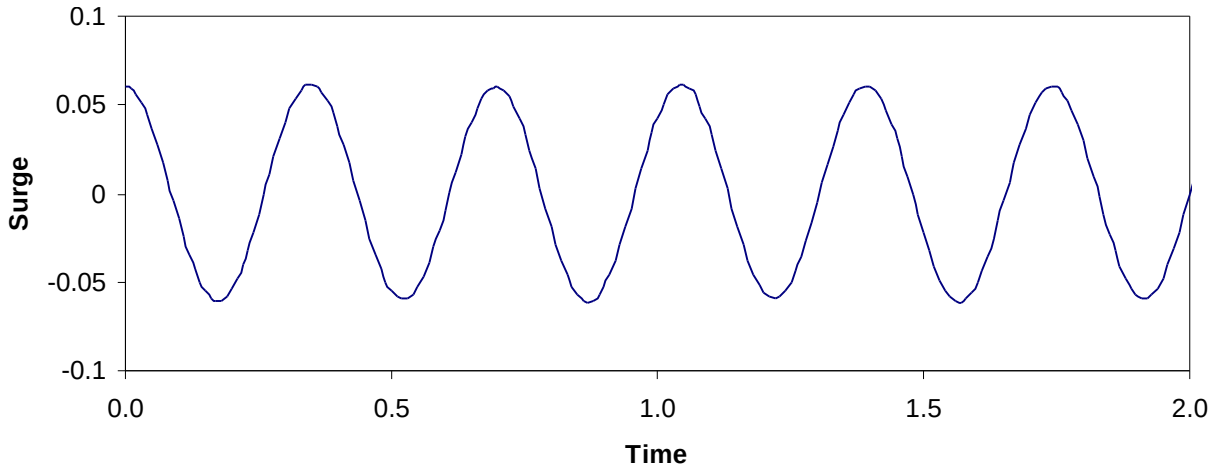

Figure 3.71. x_c, 1st Mode: Surge with Backward Pitch, x_{c_o} = 0.06

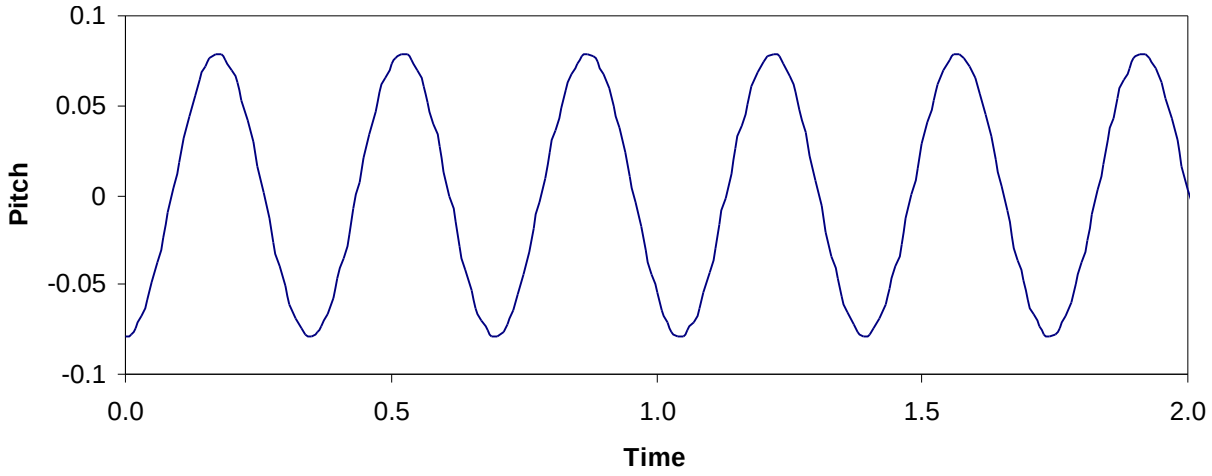

Figure 3.72. y , 1st Mode: Surge with Backward Pitch, y_o = -0.0789

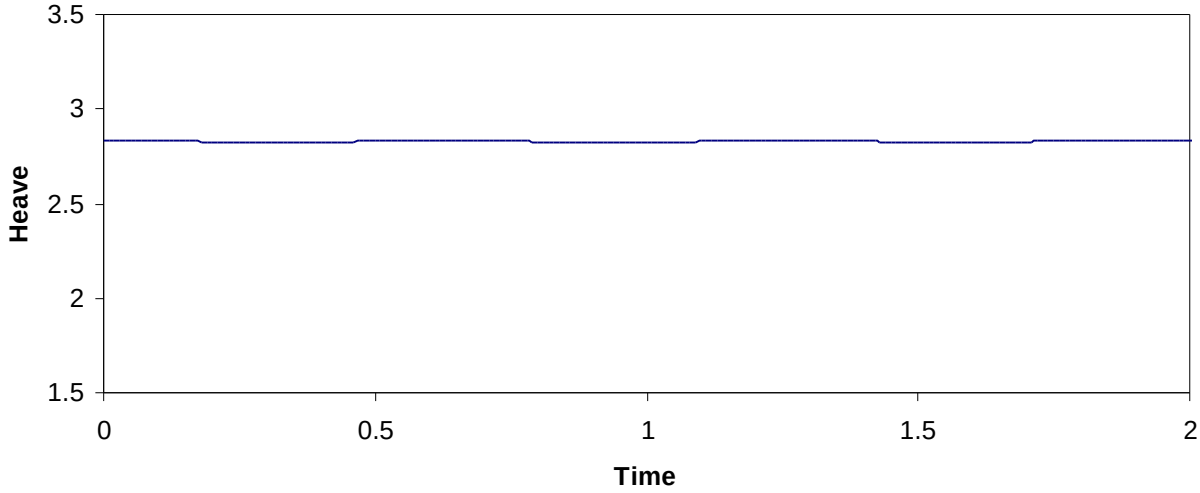

Figure 3.73. y_c, 6th Mode: Surge with Backward Pitch, $y_{c\_o} = y_{c\_eq}$

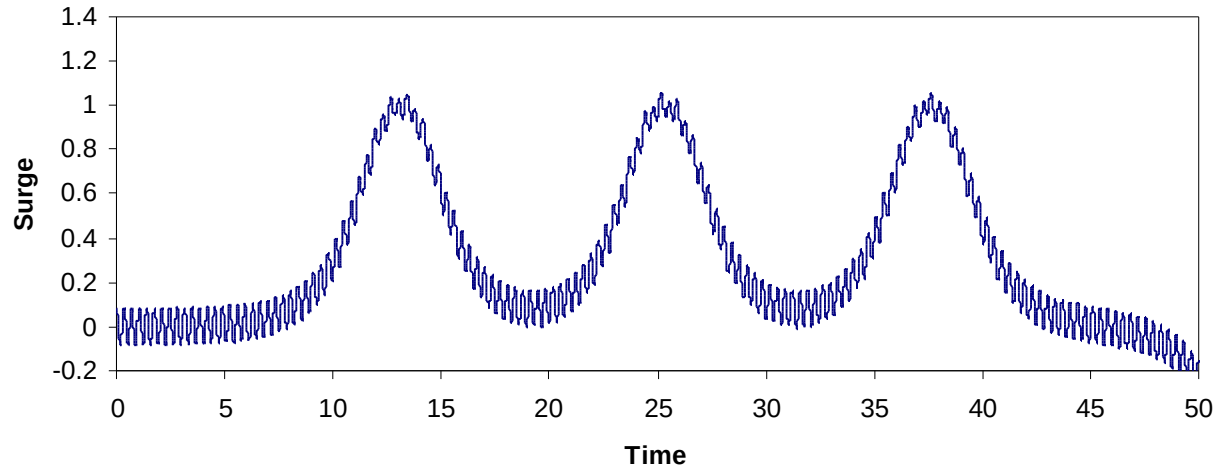

Figure 3.74. x_c, 1st Mode: Surge with Backward Pitch, x_{c_o} = 0.08

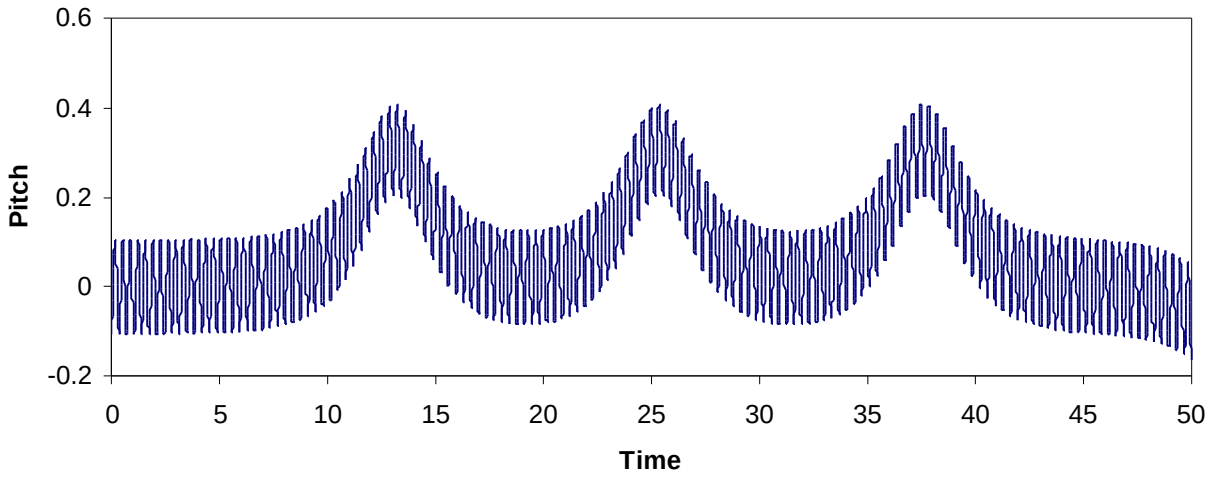

Figure 3.75. y , 1st Mode: Surge with Backward Pitch, y_o = -0.1052

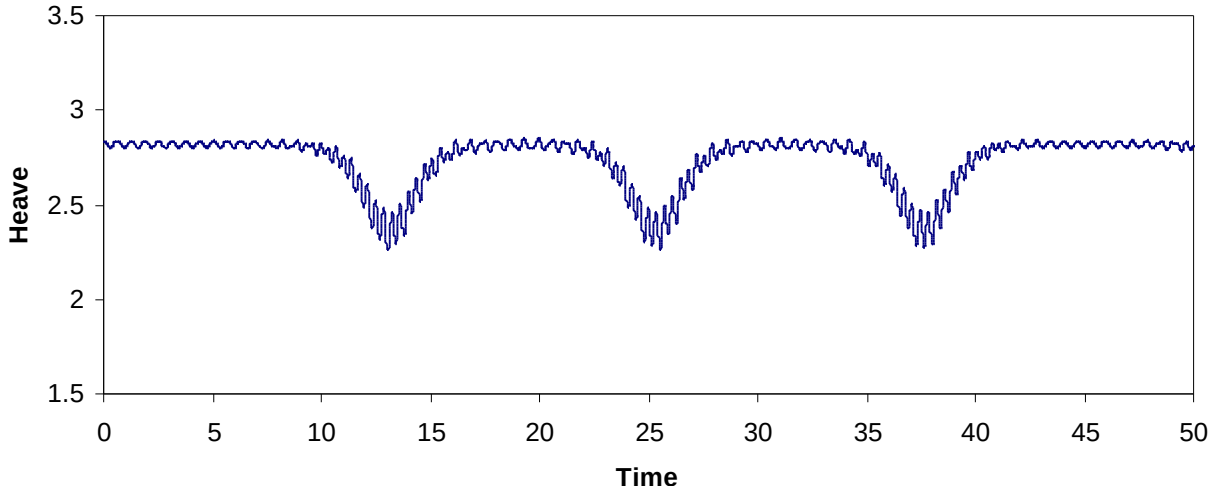

Figure 3.76. y_c, 6th Mode: Surge with Backward Pitch, $y_{c\_o} = y_{c\_eq}$

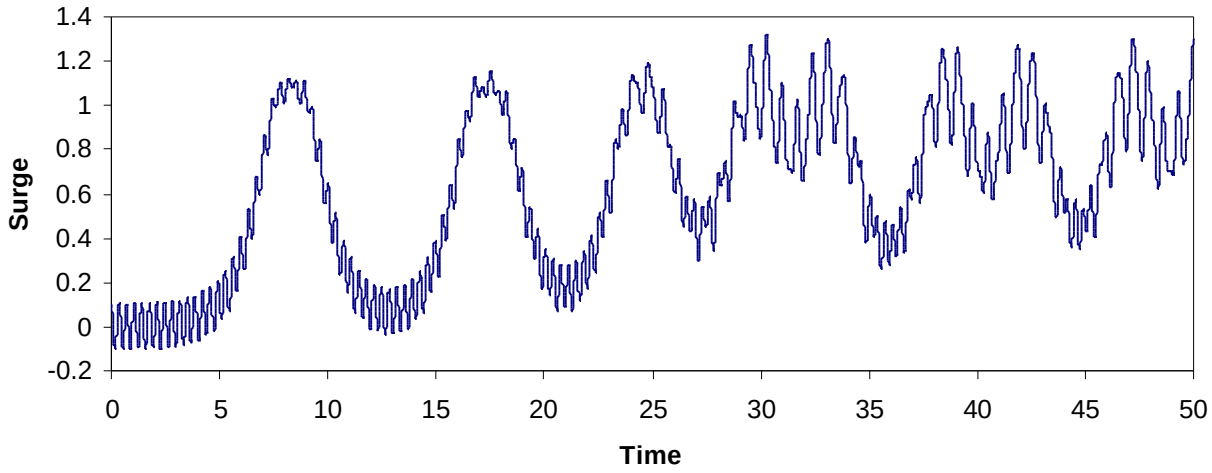

Figure 3.77. x_c, 1st Mode: Surge with Backward Pitch, x_{c_o} = 0.1

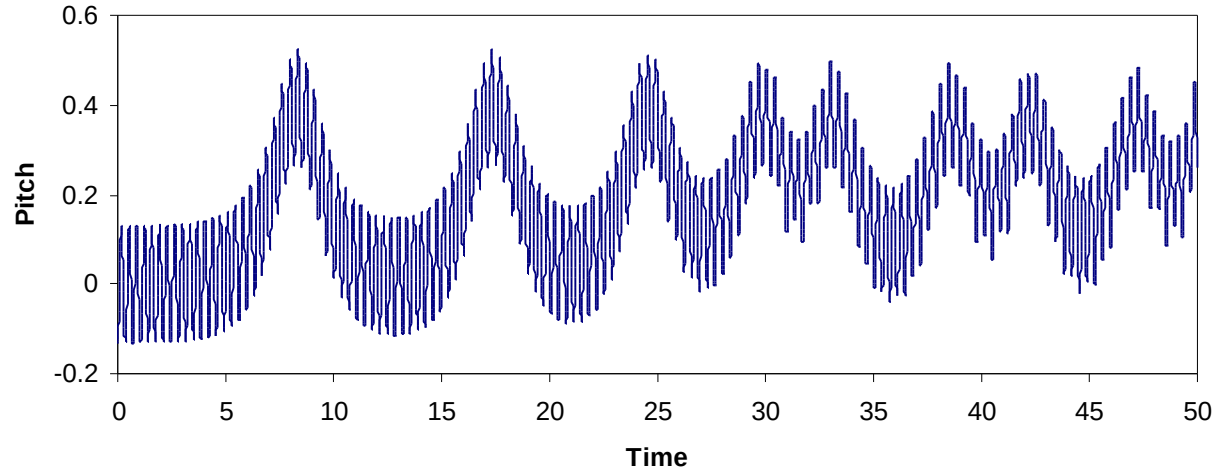

Figure 3.78. y , 1st Mode: Surge with Backward Pitch, y_o = -0.1315

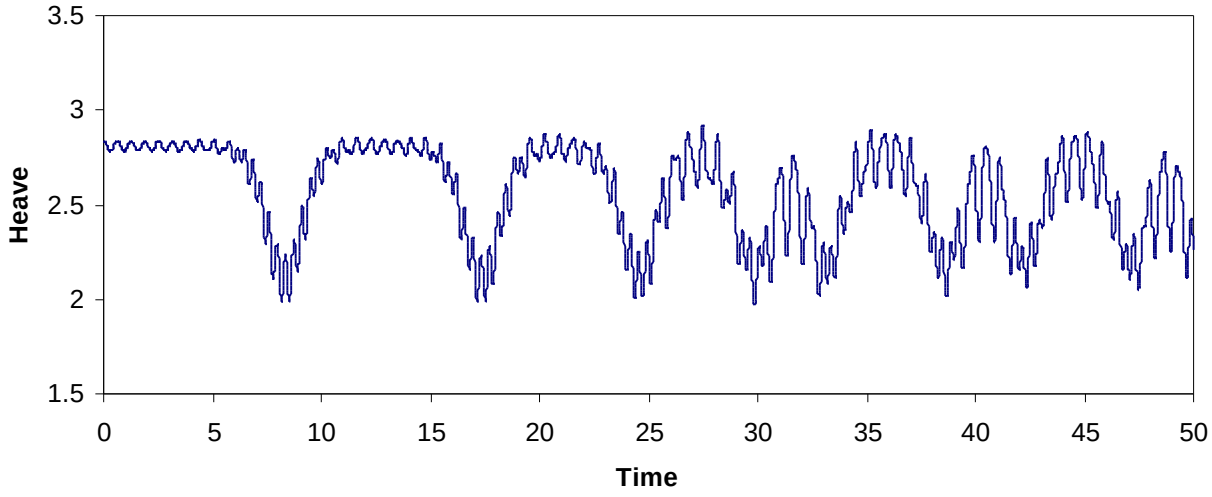

Figure 3.79. y_c, 6th Mode: Surge with Backward Pitch, $y_{c\_o} = y_{c\_eq}$

3.6 Damped Free Vibration

Until this point, undamped free vibration of the breakwater has been considered. A linear function will be used to model the fluid damping. The damping matrix, [c], will be added to the EOMs as shown in Equation 3.41:

$$[M]\ddot{\mathbf{u}} + [C]\dot{\mathbf{u}} + [K]\mathbf{u} = 0 \tag{3.41}$$

To adequately model the damping of an offshore structure, such as a breakwater, an underdamped system is necessary (Chopra, 1995). This situation occurs when, in damped free vibration, the structure oscillates about its equilibrium with a decaying amplitude.

In Figures 3.80-3.89, examples of the desired underdamped free vibration response for the six modes of vibration are presented. As the modes increase, the damping necessary to create an underdamped behavior with similar decay rate increases. For the first two modes, the value of the damping coefficient, c, used is 0.1. The damping coefficient then increases to 1.5 for the third mode, 2.0 for the fourth mode, and 3.0 for the fifth and sixth modes. Because the first and second modes are the dominant modes of vibration, the damping coefficient chosen for the standard case used for future analyses is 0.1 for each of the six EOMs.

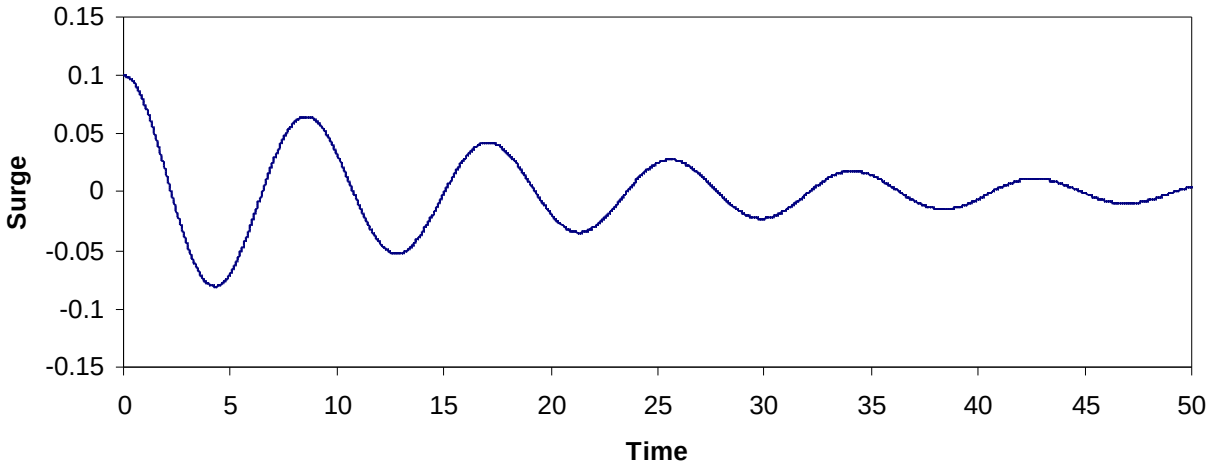

Figure 3.80. x_c, 1st Mode: Surge with Forward Pitch, c = 0.1

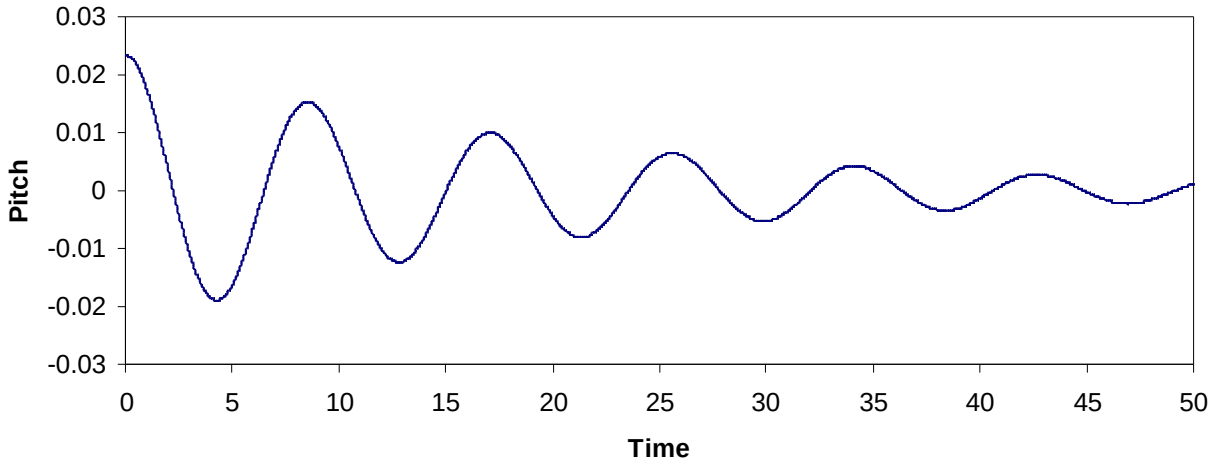

Figure 3.81. y , 1st Mode: Surge with Forward Pitch, c = 0.1

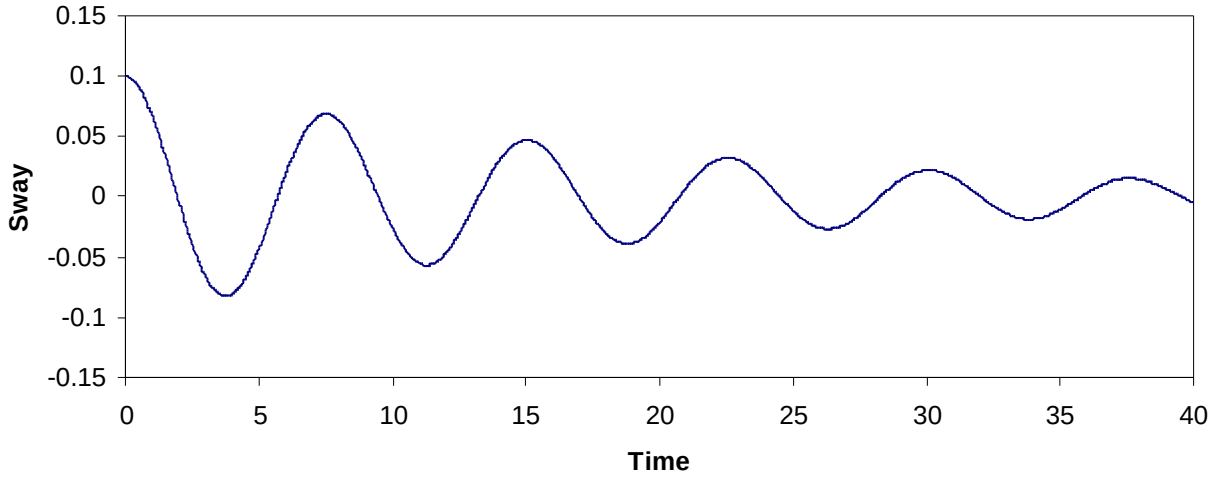

Figure 3.82. z_c, 2nd Mode: Sway with Backward Roll, c = 0.1

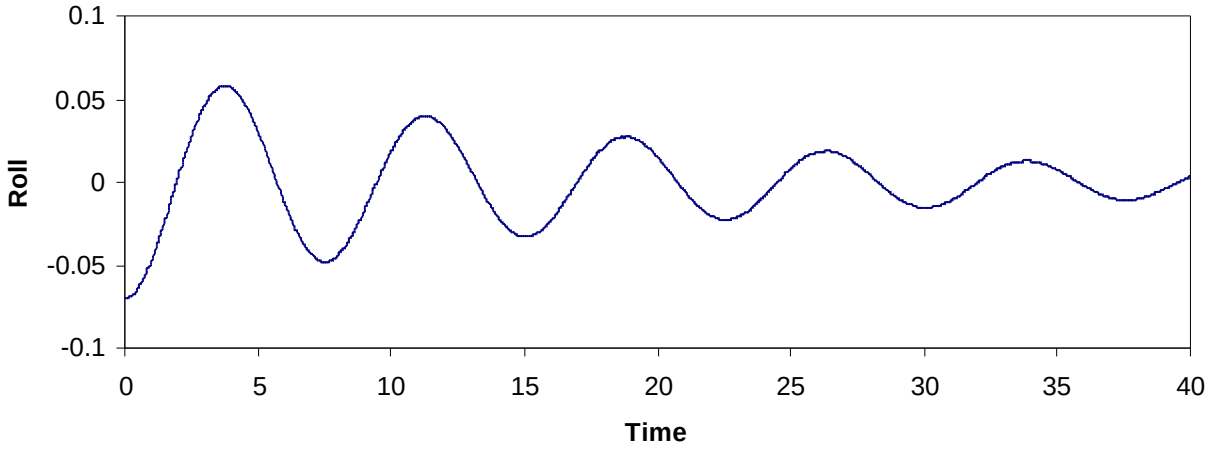

Figure 3.83. f, 2nd Mode: Sway with Backward Roll, c = 0.1

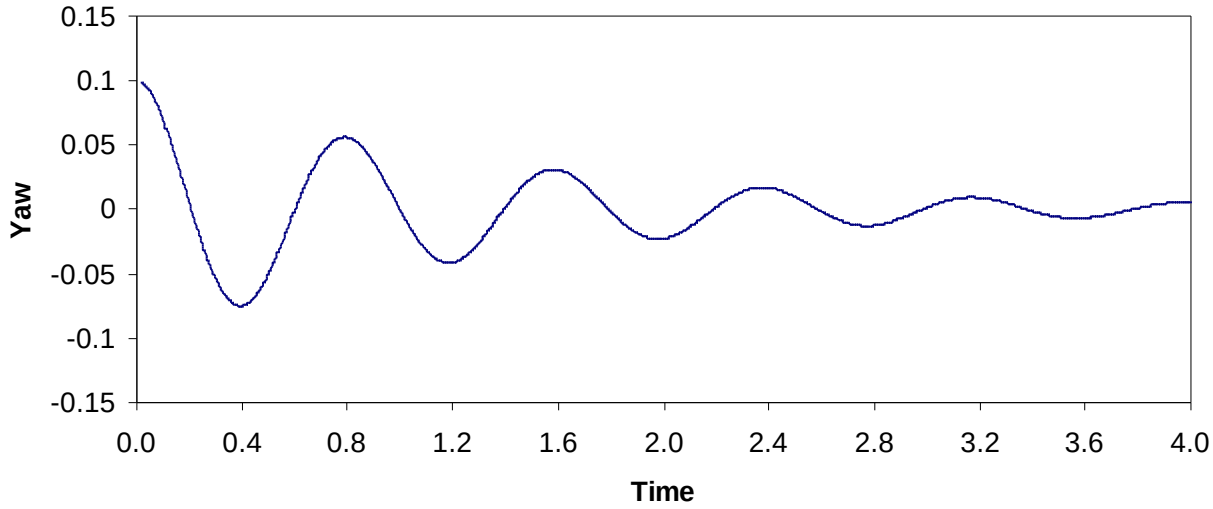

Figure 3.84. q, 3rd Mode: Yaw Only, c = 1.5

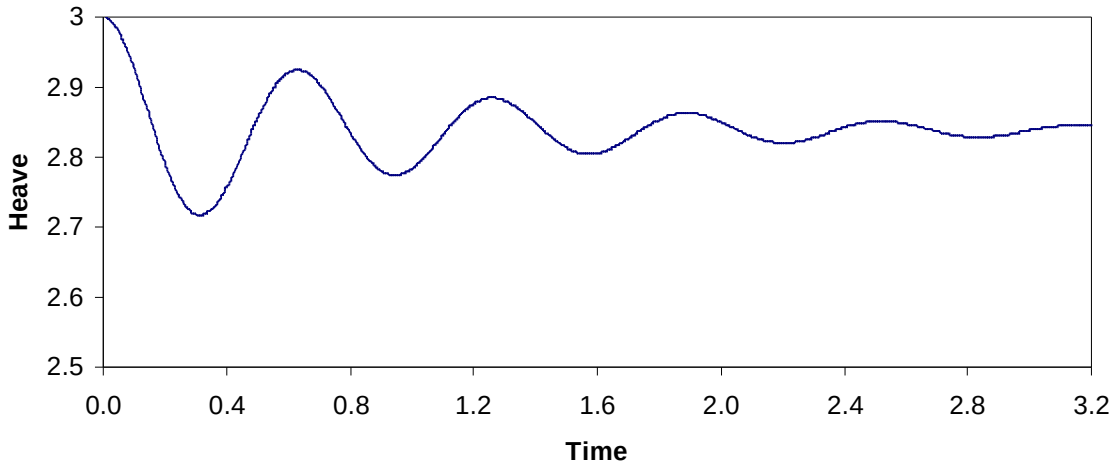

Figure 3.85. y_c, 4th Mode: Heave Only, c = 2.0

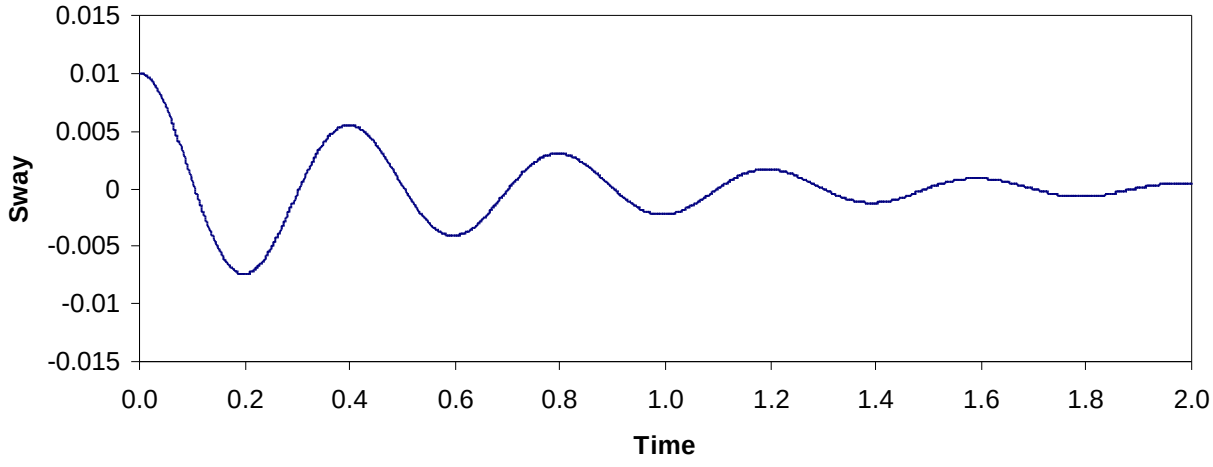

Figure 3.86. z_c, 5th Mode: Sway with Forward Roll, c = 3.0

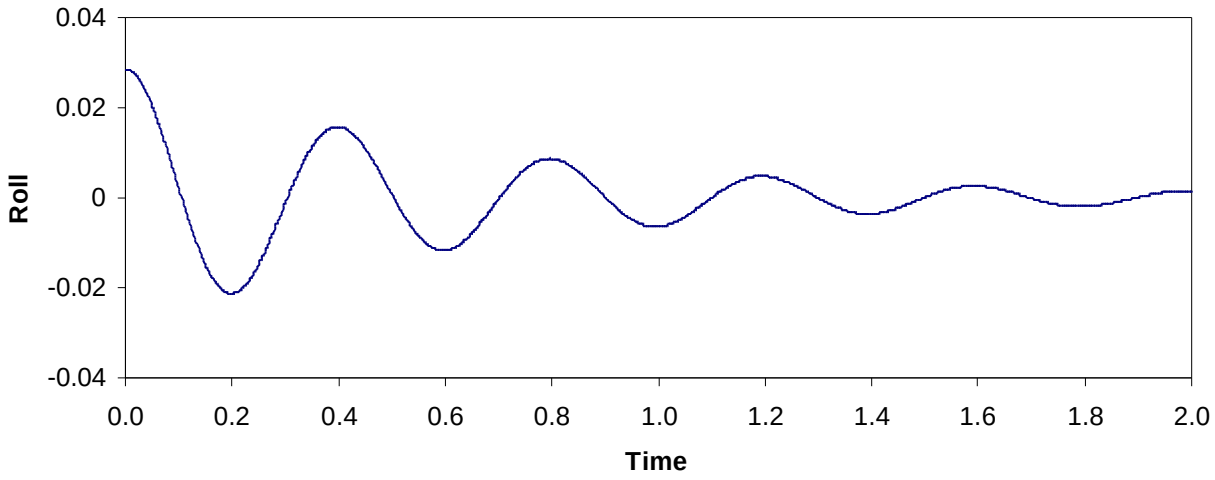

Figure 3.87. f, 5th Mode: Sway with Forward Roll, c = 3.0

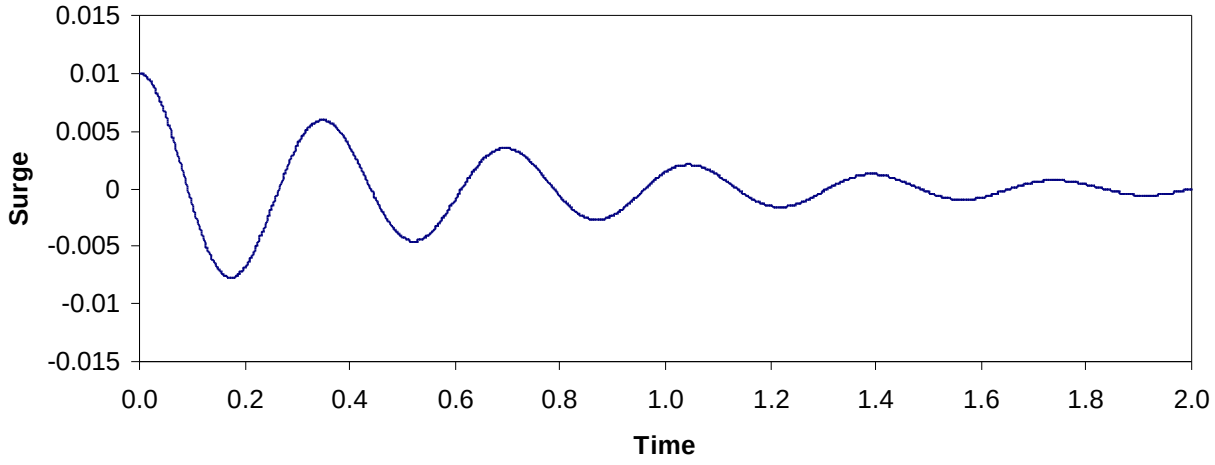

Figure 3.88. x_c, 6th Mode: Surge with Backward Pitch, c = 3.0

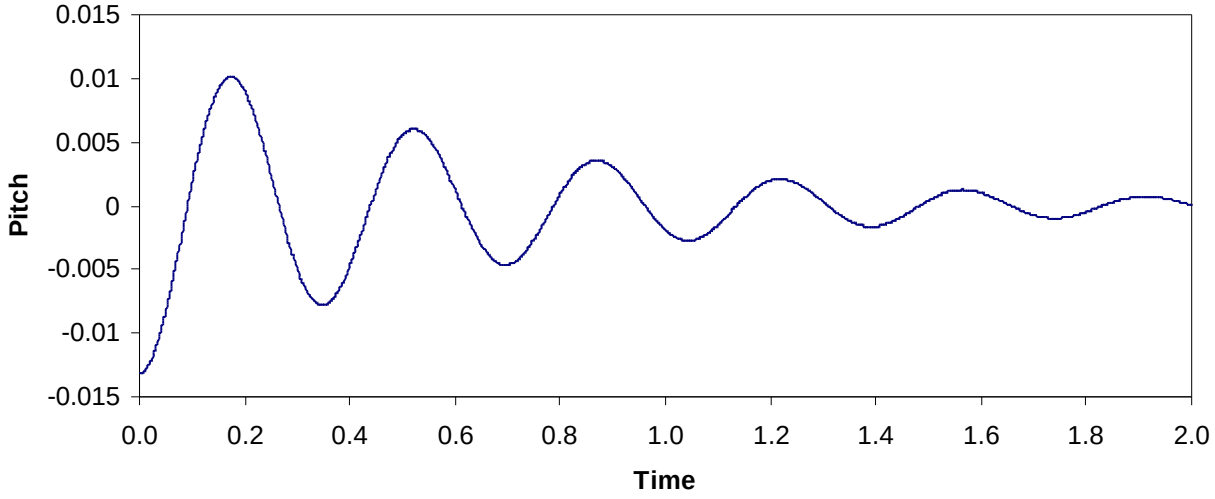

Figure 3.89. y , 6th Mode: Surge with Backward Pitch, c = 3.0